

**Islet-brain-2: a novel postsynaptic density
protein linked to an autism spectrum
disorder**

by

Joanna Giza

A dissertation submitted to the Graduate Faculty in Biology in partial fulfillment
of the requirements for the degree of Doctor of Philosophy

The City University of New York

2010

© 2010

JOANNA GIZA

All Rights Reserved

Approval Page

This manuscript has been read and accepted for the Graduate Faculty in Biology in satisfaction of the dissertation requirements for the degree of Doctor of Philosophy.

Date

Chair of Examining Committee
Dr. Mitchell Goldfarb, Hunter College

Date

Executive Officer
Dr. Laurel A. Eckhardt, Hunter College

Dr. Jesus Angulo, Hunter College

Dr. Benjamin Ortiz, Hunter College

Dr. Deanna Benson,
Mount Sinai School of Medicine

Dr. Edward Ziff, New York University

THE CITY UNIVERSITY OF NEW YORK

Abstract

Islet-brain-2: a novel postsynaptic density protein linked to an autism spectrum disorder

By

Joanna Giza

THESIS ADVISOR: Dr. Mitchell Goldfarb

Islet-brain-2 (IB2) is a neuronal protein, whose functions are not well understood. Based upon its sequence homology to JNK-interacting protein 1 (JIP1) and biochemical studies, IB2 has been described as a putative scaffold for mitogen activated protein kinase (MAPK) signaling. IB2 has been documented to interact with a wide array of functionally unrelated proteins, which has complicated efforts to confirm its biochemical role *in vivo*. In order to investigate the IB2 function in the nervous system, we have generated *Ib2* null mice. The mutants are viable and their expression of genes neighboring *Ib2* is unaffected. *Ib2* knockout mice display developmental delay in grip strength until 5 weeks (P35) of age. Their behavioral analysis following disappearance of this defect shows significant deficits in their motor learning abilities. In addition, mutant mice exhibit marked reduction in social interactions, delayed fear induced learning and unresponsiveness to the environment in various behavioral tasks. These complex atypical behaviors are reminiscent of autism spectrum disorders (ASDs). Interestingly, the human *Ib2* gene resides within the deleted chr22qter region in Phelan-McDermid syndrome and patients with this disorder manifest

similar deficits as observed in our *Ib2* null mice, suggesting that *Ib2* loss-of-function is a promising candidate model for this disorder. Recent developments in the ASDs field implicate as a major culprit defective synaptic function. Using brain fractionation and co-immunoprecipitation methods, we show that IB2 is an integral component of the postsynaptic density (PSD). Immunofluorescence shows IB2 concentrated within dendritic spine heads. *Ib2* mutation did not alter expression levels of many other common PSD components such as PSD95 and AMPA-type and NMDA-type receptors subunits. Signaling analyses conducted in *Ib2* null cultured cortical neurons failed to reveal deficits in NMDA-evoked signaling through known IB2-interacting partners TIAM1 and p38MAPK, suggesting that IB2 modulates synaptic and behavioral functions through as yet unknown molecular mechanisms.

ACKNOWLEDGMENTS

I owe my deepest gratitude to my advisor Dr. Mitchell Goldfarb for his constant support, guidance, suggestions, inspiration and helpful mentorship, without which this thesis would not be possible. It was an enormous pleasure to learn from him. He personally taught me the techniques and was always available for discussions and advice. He provided me with broad scientific training and experience. I am particularly grateful that he believed in me and allowed me to follow my ideas throughout my PhD studies. I also wish to thank my committee members: Dr. Jesus Angulo, Dr. Benjamin Ortiz, Dr. Deanna Benson, and Dr. Edward Ziff for taking their time to serve on my committee and their helpful comments and suggestions.

I also would like to thank Dr. Shirley Raps and Dr. Patricia Rockwell for their recommendation to study under Dr. Mitchell Goldfarb and for their mentorship throughout the years before and during my PhD.

I am also grateful to Hunter College's Animal Facility especially Ms. Barbara Wolin, Ms. Sonia Acevedo, Ms. Sally Sockwell and Mrs. Patricia Caldwell for the excellent mouse training I received from them and for taking wonderful care of my transgenic mouse colony.

I also wish to extend my gratitude to the former and current lab members that assisted me with my research: Dr. Bhaswati Bhandhyopadhyay, Mrs. Dafna Tchetchik, Ms. Nataly Shtraizent, Dr. Xiao Huang, Mrs. Annie Yam, and Dr. Michael Urbanski.

Finally, I would like to especially thank my beloved Henri Devedeux, who has helped me believe in myself and pursue my dreams. Many thanks to my mother Danuta Giza and my aunt Henryka Salawa for their love and continuous encouragement. Last, but not least to my wonderful daughters Annabelle and Priscilla Devedeux, who were born during my doctoral studies and were ultimately the source of my strength to complete this thesis.

TABLE OF CONTENTS

Title.....	i
Copyright.....	ii
Abstract.....	iv
Acknowledgements.....	vi
Table of Figures.....	x
Abbreviations	xiii
Chapter 1: Introduction.....	1
1.1. Protein Enzymatic Scaffolds.....	2
1.2. Synaptic Organization.....	7
1.3. Autism spectrum disorders, Phelan McDermid Syndrome, and the genetics of their etiology.....	13
1.4. Potential roles of IB2 in kinase scaffolding, synapse function, and Phelan McDermid Syndrome.....	16
Chapter 2: Materials and Methods.....	20
Chapter 3: Generation of Ib2 knockout mice.....	31
Introduction.....	31
Results.....	32
Generation of Ib2 conditional knockout mice.....	32
Generation of Ib2 full knockout mice.....	39
Necessary breeding strategies and genotyping methods.....	40
Assesment of the remaining Ib2 fragment expression in Ib2 knockout mice.....	43
IB2 knockout does not alter expression of neighboring genes.....	46

Discussion.....	49
Chapter 4: Behavioral analysis of Ib2 knockout mice.....	51
Introduction.....	51
Results.....	52
Ib2 mutation causes developmental delay in Grip strength.....	52
Motor learning and fine motor skill deficits: Rotorod assays.....	55
Reduced conditional fear learning.....	56
Deficits in social interactions.....	60
Unresponsiveness to the environment in a subset of mutant subjects.....	62
Discussion.....	68
Chapter 5: Molecular and Cellular Analysis of IB2 molecule.....	71
Introduction.....	71
Results.....	71
Generation of a mouse monoclonal antibody against IB2.....	73
IB2 presence in the brain.....	73
IB2 enrichment at postsynaptic density.....	74
IB2 associates with postsynaptic density elements.....	77
IB2 is present in dendritic spines.....	79
IB2 does not affect the basal levels of PSD components.....	79
IB2 is not essential for NMDA signaling to p38 and TIAM1.....	82
IB2 might be involved in neuronal branching.....	88
Discussion.....	89
Chapter 6: Discussion.....	92

Potential Functions of IB2 at the Postsynaptic Density.....	93
Potential Roles of IB2 in Synaptic Plasticity.....	96
Potential Functions of IB2 Beyond the Postsynaptic Density.....	97
Clinical Implications of the IB2 Knockout Behavioral Phenotype.....	98
Bibliography.....	101

TABLE OF FIGURES

CHAPTER 1

Fig. 1-1 Schematic illustration of the scaffold protein function.....	6
Fig.1-2 Schematic illustration of the postsynaptic density elements' organization at the glutamatergic synapse.	12

CHAPTER 3

Fig. 3-1 Schematic illustration of the modified mouse <i>Ib2</i> allele and IB2 protein.	33
Fig. 3-2 PCR reaction testing for the presence of CRE gene.	36
Fig. 3-3 Southern Blotting analysis of the heterozygote mice containing IB2 wild type and modified allele and expressing CRE recombinase	37
Fig.3-4 Southern Blotting analysis of the cortical cell cultures DNA derived from the IB2 ^{flox/flox} CRE ⁺ embryos.	38
Fig. 3-5 Southern Blotting analysis of the progeny following CRE microinjection into fertilized eggs.	41
Fig. 3-6 The four primer PCR reaction used to genotype the progeny from heterozygote matings.	42
Fig. 3-7a) RT-PCR analysis of IB2 expression in wild type and mutant mice.	44
Fig. 3-7b) RT-PCR analysis.	45
Fig. 3-8 IB2 is localized on murine chromosome 15 at the location 15 E3 between CHKB and ARSA genes and downstream SHANK3 gene.	48
Fig. 3-9 The growth chart of IB2 mutant, heterozygote and wild type mice.	50

CHAPTER 4

Fig.4-1 Developmental delay in grip strength.	54
Fig.4-2 Rotorod.	57
Fig.4-3 In the T-maze inhibitory avoidance test mutant mice on a mixed background show impaired learning abilities.	59
Fig.4-4 Mutant animals show reduction in social interactions.	61
Fig.4-5a Nonresponsive phenotype in the subset of mutant mice in one way escape in T-maze apparatus.	64
Fig.4-5b Nonresponsive phenotype in the subset of mutant mice in Novel Object Recognition test.	65
Fig.4-5c,d Nonresponsive phenotype in the subset of mutant mice in open field and dark and light paradigm assays.	67

CHAPTER 5

Fig.5-1 Protein extracts were prepared from different brain regions of a wild type mouse...75	75
Fig.5-2 Brain fractionation shows co-enrichment of IB2 with postsynaptic density elements.....76	76
Fig.5-3 IB2 co-immunoprecipitates with postsynaptic density elements78	78
Fig. 5-4 Rat hippocampal neurons immunofluorescence80	80
Fig.5-5 IB2 (green) can be found in spine heads (indicated by arrowheads) where it colocalizes with actin (red)81	81
Fig.5-6 The basal levels of postsynaptic density constituents are unaffected in IB2 knockout Mice83	83

Fig.5-7 The levels of NMDAR subunits in cerebellum are unaffected in IB2 knockout mice

Brain84

Fig.5-8a) The levels of basal and activated p38 MAPK kinase in wild type and mutant culture following NMDAR induction are the same.86

Fig.5-8b) The basal levels of p38 and phosphor- p38 in the brain at different developmental stages: adult (P60) and pup (P14) also do not differ.86

Fig.5-9 TIAM1 induction in cortical cultures prepared from wild type, heterozygote and mutant embryos.87

Fig.5-10 Golgi staining of Purkinje neurons in a three week old wild type and knockout mice.100

ABBREVIATIONS

- ABP1** AMPARs binding protein
- AMPA** α -amino-3-hydroxyl-5-methyl-4-isoxazole-propionate
- APV** (2*R*)-amino-5-phosphonovaleric acid (NMDAR antagonist)
- ARSA** arylsulfatase A
- ASD** autism spectrum disorder
- CAD** catecholaminergic-A-differentiated cells
- CAMKII** Ca²⁺/calmoduline kinase II
- Chkb** choline kinase beta
- CNQX** 6-cyano-7-nitroquinoxaline-2,3-dione (AMPA antagonist)
- Cre** Cyclization Recombination
- Cy5** Cyanine 5
- DIV** day in vitro
- DSMV-IV** Diagnostic and statistical manual of mental disorders IV
- eEF2K** Eukaryotic elongation factor-2 kinase
- ERKs** extracellular regulated kinases
- FITC** Fluorescein isothiocyanate
- FHF** Fibroblast growth factor homologous factor
- Floxed** flanked by LoxP
- FSH** follicle stimulating hormone
- GABA** gamma-aminobutyric acid
- GluR** glutamate receptor
- GRIP** glutamate receptor interacting protein
- GPCR** G-protein coupled receptor
- GUK** guanylate kinase domain

hCG human chorionic gonadotropin hormone

IB1 islet brain 1 protein

IB2 islet brain 2 protein

IP Immunoprecipitation

JBD JNK binding domain

JIP JNK interacting protein

JNK c-Jun N-terminal kinase

KSR kinase suppressor of RAS

LoxP locus of X-over P1

LTD long term depression

LTP long term potentiation

mGluR metabotropic glutamate receptor

MAGUKs membrane associated guanylate kinases

MAPK mitogen activated protein kinase

MKK mitogen activated protein kinase kinase

MLK mixed lineage kinase

MUPP1 multiple PDZ domain protein

NMDA N-methyl-D-aspartic acid

PGK phosphoglycerate kinase

PCR polymerase chain reaction

PDZ post synaptic density protein (PSD95), Drosophila disc large tumor suppressor (DlgA), and zonula occludens-1 protein (zo-1) domain

PFA paraformaldehyde

PKA protein kinase A

PMSG pregnant mare serum gonadotropin

PSD postsynaptic density

PTB phosphotyrosine binding domain

RT-PCR reverse transcriptase polymerase chain reaction

SAM sterile alpha motif domain

SH3 Src homology 3 binding domain

SHANK3 SH3 and multiple ankyrin repeat domains 3 protein

SYN synaptosomes

TIAM1 T-cell lymphoma invasion and metastasis 1

TPR tetratricopeptide repeat motif

TTX tetrodotoxin

CHAPTER 1

INTRODUCTION

Complex animal behaviors are governed by higher order functions that require signaling within neural networks. At the center of the faithful transmission of this information lays the synapse. My research has focused on poorly understood islet brain 2 (IB2) molecule considered to be a putative scaffold protein. I have shown that IB2 is a synaptic component whose function is necessary for an animal's performance of complex behaviors. Of particular interest is the connection of IB2 deficits and autism spectrum disorders with specific similarities to Phelan-McDermid Syndrome. As a background for this multidisciplinary dilemma, my thesis introduction is composed of seemingly unrelated sections including protein enzymatic scaffolds, synaptic organization and autism spectrum disorders followed by possibilities for their connections with IB2.

1.1. Protein Enzymatic Scaffolds

All eukaryotic cells undergo biochemical signal transduction in response to signals coming from their local environment. Many diverse stimuli trigger signaling through evolutionary conserved mitogen activated protein kinase (MAPK) cascades that regulate cellular fate, influencing processes including cell division, gene activation and apoptosis. These cascades are based on a three geared command system of sequentially activating protein kinases that participate in a signal transduction. Each MAPK is phosphorylated and thus activated by one or more MAPK kinases (MAPKKs), which in turn are being activated by MAPKK kinases (MAPKKKs). This process is believed to result in the signal amplification (Gallo and Johnson, 2002). Mammalian MAPKs are composed of three major groups: extracellular regulated kinases (ERKs), c-Jun NH2 terminal kinases (JNKs) and p38s, which can be further divided into isoforms. Generally speaking each group has an ascribed function related to common type of responses such cell division for ERKs, stress for JNKs and inflammation for p38s (Johnson and Lapadat, 2002; Roux and Blenis, 2004). However, recent data suggests their involvement in many more specific processes depending on the cell type and incoming signal. Nevertheless, it is difficult to imagine how this group of molecules could respond to the different stimuli and elicit very specific and appropriate responses at the right time and location. One very plausible possibility is the presence of the scaffold proteins.

Many scaffolds have been described to date, although an understanding of their functions is still in its infancy. The yeast Ste5 is the first described and most extensively studied scaffold (Elion, 2001). Among many mammalian scaffolds are KSR for ERK and JIPs for JNK and p38 signaling, although these scaffolds are less understood (Burack and

Shaw, 2000; Burack et al., 2002; Gallo and Johnson, 2002; Kelkar et al., 2005; Whitmarsh et al., 2001). There is no sequence homology between yeast and mammalian scaffolds, but they do share certain characteristics that allow for uniting them under a common scaffolding umbrella (Fig.1-1).

One of the most important features of a scaffold is to concentrate and bring together sequentially acting pathway components (Burack and Shaw, 2000; Burack et al., 2002; Flatauer, 2005). For instance Ste5 interacts with Ste7 MAPKK and its upstream activator Ste11 MAPKKK and downstream effector MAPK Fus3 (Burack et al., 2002; Elion 2001). JIP1 interacts with JNK, its upstream kinase MKK7 and its activator MLK3 (Yasuda, 1999; Whitmarsh 2001). By holding these kinases together, the scaffolds not only allow the signal transmission, but also prevent them from being utilized in other pathways that may require the same enzymes (Flatauer, 2005; Good et al., 2009). Due to these properties, it is crucial that the levels of scaffolds are carefully produced and maintained by the cell. Otherwise, too much of a scaffold could sequester single components, thus preventing the signal transmission and too little would be of no help (Ferrell 2000). Consistent with this reasoning are the findings showing that the scaffold overexpression *in vitro* or in cells leads to signal transduction inhibition (Burack 2000; Burack et al., 2002; Yasuda 1999). It is not exactly clear whether the scaffolds exist in complexes with cascade components in a steady state or they are being assembled in response to the signal. It has been shown for JIP1 that small amounts of sequentially acting enzymes precipitate with the scaffold, but the levels of these complexes are significantly increased upon the pathway activation (Whitmarsh 2001). Currently, two models have been proposed for scaffold functioning. One assumes the existence of transducisome composed of a scaffold and bound sequentially acting kinases as is the case for Ina D scaffold in drosophila that participates in photoresponses (Burack 2002).

The other model, proposes free diffusion of the signaling components, which permits a “switch-like” response that helps to eliminate the noise (Burack, 2002; Ferrell 2000).

Regardless of the model, however, they both argue that the presence of a scaffold limits the signal amplification used to be believed to be the goal of a multistep signaling (Burack 2000; Burack et al., 2002). Instead, the scaffold is thought to ensure the specificity, which seems to be another important role of this group of proteins. For instance, in yeast MAPKKK Ste11 can be activated by three different and unrelated stimuli such as osmotic stress, starvation and pheromone (Elion 2001; Flatauer 2005). Starvation and pheromone signals also share downstream MAPKK Ste7, which then can choose between MAPK Kss1 or Fus3 which are downstream effectors of these two pathways respectively. It has been shown that Ste5 scaffold is responsible for conveying specificity to the mating pheromone pathway (Flatauer 2005; Good 2009). It is expressed only in haploid cells designated for the process of mating (Elion 2001) and in strains lacking Ste5 where Ste11 MAPKKK is constitutively active only Kss1 MAPK is activated (Good 2009).

These findings highlight another important function proposed for scaffolds, which is their catalytic ability. It is thought that by binding to sequential components scaffold allows for kinases to have a fast and easy access to their downstream targets. Ste5 was found to actually catalytically “unlock” the Fus3 MAPK thus changing it into a very good substrate (Good et al., 2009). In addition, it operates as a dimer, thus possibly allowing for a proper alignment of signal transduction components which leads to fast phosphorylation events (Good et al., 2009). Interestingly, JIP molecules have also been found to form homo and oligomeric complexes (Yasuda 1999). Not to mention that the MAPKs and their upstream activators are also regulated by dimerization, necessary to remove the autoinhibition since many of them

have a domain bound to or masking their enzyme active site in an inactive state (Gallo and Johnson 2002).

Scaffolds are also believed to serve as adaptors or anchors that bring the signaling components to the plasma membrane region where the signal is being received (Flatauer, 2005). JIP molecules, for instance, are known to interact with the motor protein kinesin, that is thought to help in their delivery to the ends of the cells like neurons including distinct polar regions such as axon and dendrites. Similarly, Ste5 has also been shown to interact with cell polarity elements, which could make it more recruitable to the specific location at the cell membrane. Additionally, Ste5 interacts with the G $\beta\gamma$ subunit of G protein coupled receptor after its diffusion from trimeric G protein following pheromone induction, thus bringing the signaling pathway to the membrane vicinity (Elion 2001; Flatauer, 2005).

Last, but not least, scaffolds are both cytoplasmic and nuclear. Ste5 experiments in yeast indicated that it is necessary for the scaffold to enter the nucleus in a process so called “nuclear shuttling”. It is thought that in the nucleus the scaffolds associate with the MAP kinase and its upstream activator MAPKK and possibly cell polarity molecules (Elion 2001). As a result, mating yeast undergo chemotactic growth towards the pheromone signal. Also of interest, the scaffold JIP1 which is normally found at the axonal and dendritic tips, is seen as puncta in the nucleus following JNK pathway activation (Whitmarsh 2001). It is not known whether the activating signal leads to increased export or a rate of export of the nuclear scaffold in yeast or actual transport to the nucleus as it might be the case for JIP1. Regardless whether it is an export from or import to or possibly both, the passage through the nucleus seems to be an important and necessary characteristic of some scaffolds either for their association with specific proteins or gene expression activation.

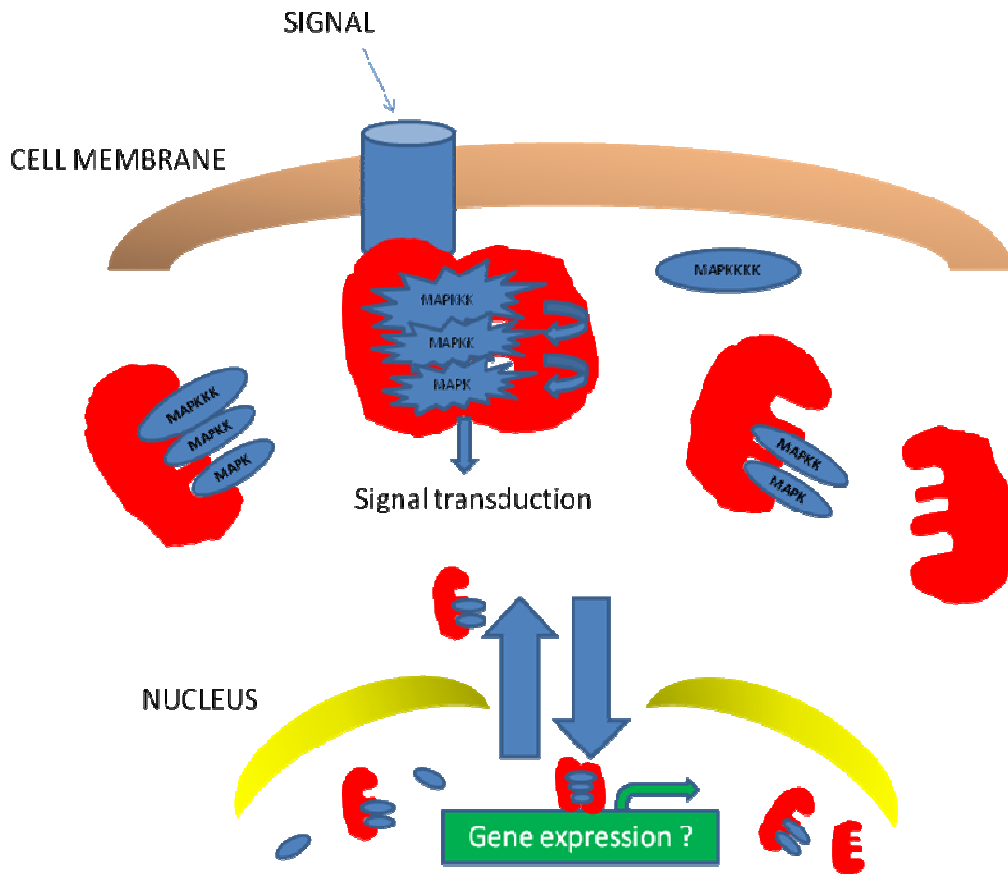


Fig.1-1 Schematic of the scaffold protein functions. Upon signal activation of the receptor, a scaffold is recruited to the plasma membrane. It brings sequentially acting kinases of the MAPK pathway in close proximity to the signal, thus allowing its transmission and conveying specificity. Scaffolds are believed to function as dimers, which is believed to activate the catalytic properties of the kinases. Scaffolds are both cytoplasmic and nuclear. It is possible that upon signal activation of the receptor, scaffolds travel to the nucleus where they participate in gene expression. For instance, upon signals resulting in JNK activation, JIP1 normally found at the end of neuronal projections is observed as puncta in the nucleus. Alternatively or in addition to, the “nuclear shuttling” makes the kinase more recruitable to the plasma membrane as it is the case for the yeast Ste5. It is possible that in the nucleus the scaffolds interact with other MAPK cascade components, which are also both cytoplasmic and nuclear and/or generate scaffold dimers that can now bind to the receptor. Furthermore, they may associate with other necessary molecules. The receptor induction may then also activate the export or enhance the rate of the export of such activated scaffold, thus allowing a proper signal transmission.

1.2. *Synaptic Organization*

The nervous system governs every sensory, motor, and behavioral aspect of an organism calls for extremely well organized and controlled communication center. While the glia take upon themselves the support in terms of structure, nutrients and cleaning, the neurons are in charge of receiving, processing and sending out the information (Garner and Nash, 2001; Kandel et al., 2000). This critical role determines the highly specialized structure of neuronal cells. They are strongly polarized cells composed of multiple dendrites that in general receive input signals, which are then transmitted and processed in cell body with residing nucleus and subsequently sent out through an axon as action potentials to target cell(s). The end part of an axon called an axonal swelling or presynaptic bouton forms a connection with the postsynaptic site at the dendritic swelling called the synapse named from a Greek word “to clasp” (Garner and Nash, 2001). The synapse is a meticulously organized unit since the faithfully and precisely transmitted and received information is critical for a proper functioning of the entire organism. An average neuron possess ~1000 synaptic connections whereas a Purkinje cell which is the most arborized neuron in the nervous system can have as many as 100,000 (Kandel et a;., 2000). The intricate connections of the dendritic and axonal networks usually result in the synapses formed between an axon and dendrite (axodendritic), or the specialized extensions of the dendrites called spines, but they can also happen between two axons (axoaxonal), two dendrites (dendrodendritic) or even an axon and the soma or a region of an axon called axon initial segment (Garner and Nash., 2001). The morphology and the structure of a neuronal cell allows for a transmission of an electrical and chemical signal. While electrical synapses serve to transmit simpler and rapid signals, the chemical ones can

elicit more complex and long lasting responses in the nervous system that result in more complex behaviors (Kandel, et al., 2000).

The chemical synapse is composed of three well connected, but structurally and functionally distinct regions: pre and postsynaptic terminals separated by the synaptic cleft. It transmits signal in the form of a chemical neurotransmitter, which is released by presynaptic terminals into the synaptic cleft and binds to the receptor at the postsynaptic site. Depending on the nature of the neurotransmitter, the synapses can be divided into inhibitory and excitatory. The most common neurotransmitters are amino acids or derivatives, such as inhibitory GABA, inhibitory glycine and excitatory glutamate (Kandel et al., 2000; Garner and Nash, 2001). Neurotransmitters are stored in synaptic vesicles residing at the presynaptic bouton as a reserve pool or as ready for release docked at the membrane at so called active zone. As the action potential, electrical impulse, generated in the dendrite travels down the axon, it results in opening of the voltage gated calcium channels at the presynaptic sites. Calcium influx through these channels results in the fusion of the vesicles with the plasma membrane and neurotransmitter release into the synaptic cleft. Neurotransmitters can then be recycled in the process of clathrin mediated endocytosis, brought back by the transporters or synthesized *de novo* (Garner and Nash, 2001; Kandel et al., 2000). Released neurotransmitters diffuse into the synaptic cleft localized between pre- and post-synaptic terminals. This specialized compartment is small enough to allow the neurotransmitter to quickly reach the postsynaptic receptors. Unbound or dissociated neurotransmitter is cleared from the cleft by diffusion, degradation, or presynaptic reuptake transporters. This clearance protects from prolonged or a toxic effect on the postsynaptic site. In general, it also prevents neurotransmitter diffusion to the neighboring synapse, although the spillover events have been described. Synaptic cleft is composed of extracellular matrix molecules, cell adhesion

molecules and metalloproteases that regulate the cell-cell adhesiveness (Bourne and Harris, 2007; Garner and Nash, 2001). The signaling molecules at the junction are believed to determine what types of receptors are clustered at the postsynaptic site. This review will further focus on the postsynaptic region typical of the excitatory glutamate synapse.

The postsynaptic site contains a specific region called postsynaptic density (PSD) named after the opaque stained region revealed through electron microscopy. In addition to the dendrite itself, an overwhelming majority of the excitatory synapses is localized at the spines. These small dendritic protrusions often contain a long, thin neck and head, and can be divided based on their morphology into stubby, thin and mushroom like (Bourne and Harris, 2007 and 2008). The PSD is localized in the spine head. It is composed of the glutamate receptors, molecules of the cytoskeleton, and the adaptors that connect them together (Bourne and Harris, 2007 and 2008). The glutamate receptors can be divided into metabotropic (mGluR) G protein coupled (GPCR) receptors and ligand gated ion channels that include AMPA, NMDA and kainate receptors. The slower responding mGluRs act via second messenger system and can lead to excitatory or inhibitory responses through their modulation of other channels by phosphorylation or dephosphorylation events. Since the other receptors are ion channels that open in response to ligand which is a glutamate, their actions are much faster (Kandel et al., 2000). Kainate receptors are not very well described whereas NMDA and AMPA receptors are the most studied of the glutamate receptor family. NMDARs are composed of NR1 and NR2A-D subunits. NR1 and NR2 subunits form the glutamate binding site. In addition, NMDARs also require the cofactor glycine for proper functioning. They are normally inactive due to the presence of Mg^{+2} ion within the channel pore, which is removed during depolarization event. NMDARs are permeable to calcium, sodium and potassium ions. However, their contribution to cell depolarization is relatively

small and their crucial role is related to the calcium entry, which then can trigger activation of multiple signal transduction pathways. AMPARs on the other hand are the major channels involved in depolarization events at the postsynaptic site. They can be composed of GluR1-4 subunits and operate as double dimers. AMPARs are co-permeable to sodium and potassium, hence, their contribution to depolarization. However, the absence of GluR2 subunit can convey permeability to calcium. During synaptic transmission, the action potential at the presynaptic terminal results in the glutamate release and AMPAR activation and thus depolarization of the postsynaptic region. This allows for the removal of magnesium ions from NMDARs, thus activating them. If the second signal arrives at that site, it causes calcium influx through NMDARs and the activation of various signal transduction pathways (Garner and Nash, 2007 and 2008; Kandel et al., 2000; Bourne and Harris, 2007). One of the major events occurring at the synapse in which glutamate receptors participate is synaptic plasticity during learning and memory formation. Plasticity produces a change in the signaling strength at the given synapse as a result of the synaptic activity. There are two types of the synaptic plasticity: long term potentiation (LTP) and long term depression (LTD). As their names suggest, they are involved in either potentiation or depression of a given synapse strength respectively. The calcium flow through NMDARs triggers activation of multiple kinases such as CAMKII, PKA, MAPK and aurora kinases. These kinases can modify the existing AMPARs by phosphorylation, thus regulating their permeability to sodium and can also mediate transit of AMPARs between intracellular vesicles and the postsynaptic membrane, either increasing or decreasing receptor density in LTP and LTD, respectively (Bourne and Harris, 2008). More persistent activation of postsynaptic kinases can induce new protein synthesis through either new gene expression or translation of prior dormant dendritic mRNAs, thereby inducing longer lasting changes in synaptic architecture

and connectivity and in density of postsynaptic neurotransmitter receptors (Bourne and Harris, 2008).

The postsynaptic density is a large network of interacting proteins that include multivalent scaffold proteins along with membrane receptors, which is further anchored to the underlying cortical actin cytoskeleton in the dendritic spine. Three families of PSD scaffolding proteins have been described. One of them includes the proteins composed solely of PDZ domains such as glutamate receptor interacting protein (GRIP) AMPARs binding protein ABP1, and multiple PDZ domain protein MUPP1 (Garner and Nash, 2001). The second family includes proteins composed of PDZ, SH3 and GUK domains that contain membrane associated guanylate kinases (MAGUKs) such as PSD95 that interacts with NMDARs. The third family called Prosap/SHANK proteins have an ability to interact with the above families in addition to Homer, an mGluR-binding protein, thus holding and organizing all classes of glutamate receptors at the postsynaptic density (Bourne and Harris, 2007 and 2008; Garner and Nash, 2001; Sheng, 2000). The stability and structure of the PSDs are crucial for the proper neurotransmission and neuronal plasticity during memory and learning processes. In addition, many neurological diseases have been attributable to malfunctioning of the PSD components.

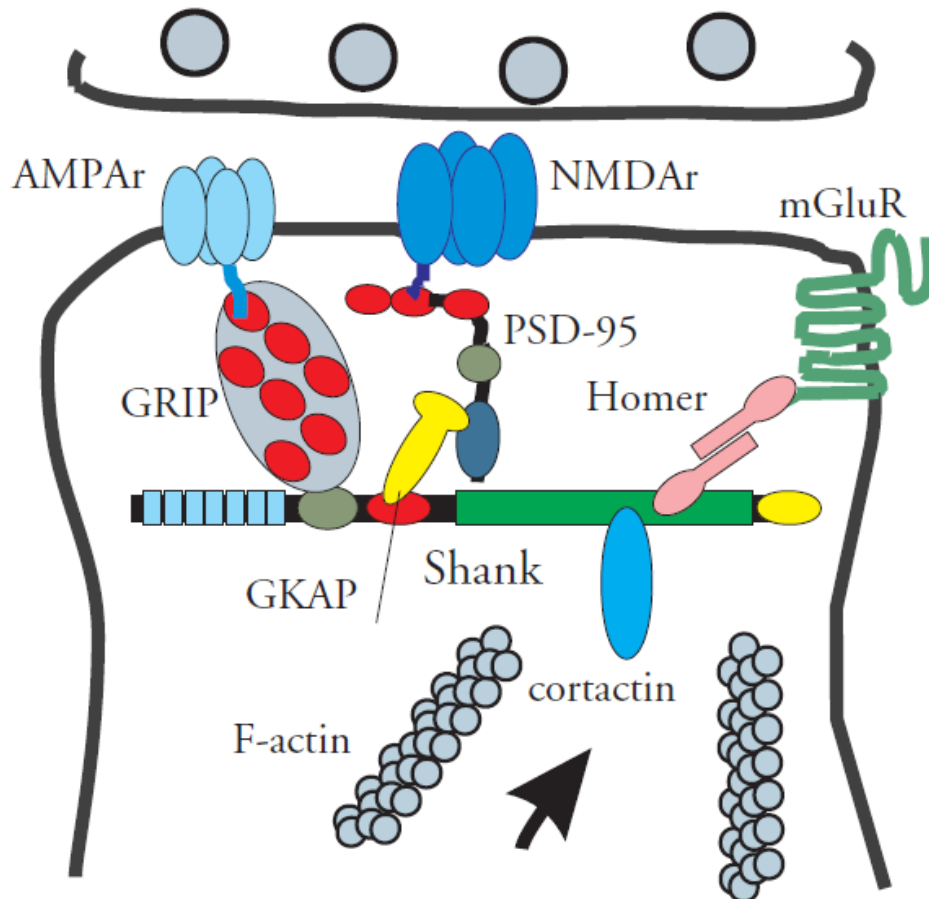


Fig.1-2 (Reprinted from Sheng et al., 2000)
 Schematic illustration of the postsynaptic density elements' organization at the glutamatergic synapse.

1.3 Autism spectrum disorders, Phelan McDermid Syndrome, and the genetics of their etiology

Autism spectrum disorders (ASD) include autism, Rett's syndrome, Asperger's syndrome, and Childhood Disintegrative disorder. Affected individuals display deficits in social interactions, difficulties communicating either through language or appropriate gestures, and nonresponsiveness to environment. These individuals often preoccupy themselves with details of objects and engage in stereotypic behaviors. Other characteristics of these disorders may include some level of mental retardation, sensory deficits or even seizures. The degree and onset of these symptoms differ among affected individuals. For instance a child may achieve developmental milestones on schedule until a certain age (12-24 months) after which further acquisition of social and/or language skills may be impaired, and prior acquired skills may regress. In other instances, alarming characteristics may be observed very early on after birth (*Diagnostic and statistical manual of mental disorders: DSM-IV*; Zoghbi, 2003; Walsh et al., 2008 <http://www.nimh.nih.gov/health/publications/autism/complete-index.shtml>).

Phelan-McDermid Syndrome, also termed 22q13 Deletion is another recently described disorder with autistic like features and characterized by deletions in the terminal region of chromosome 22 (22q13). The symptoms include unresponsiveness to the environment during the first few months of life, repetitive behaviors, sudden loss of once mastered skills and a delayed, poor or absent language acquisition. In addition to ASD-like symptoms, the hypotonia, impairment of fine and gross motor skills, difficulty processing sensory information and some level of social interactions later in development are also observed. Similarly to other ASDs, the degree and extent of phenotypic features differs among patients and early similarities lead to misdiagnosis of autism (Philippe et al., 2008; Wilson et al., 2003). One of the missing genes in all the patients is *Shank3*. A few other examples of autism

bearing associated point mutations at the *Shank3* locus have suggested that SHANK3 loss of function may cause Phelan-McDermid syndrome along with other ASDs. SHANK3 organizes molecules in the cytoplasm at the postsynaptic density, suggesting that synaptic disorganization could underlie behavioral dysfunction (Wilson et al., 2003; Sheng 2000). However, it is not clear whether other genes neighboring *Shank3* may also contribute to Phelan McDermid syndrome. It appears that many of the genes implicated in autism also correspond to synaptic proteins (Zoghbi, 2003). For instance, a mutation of *mecp2* encoding a protein that regulates density of glutamatergic synapses has been shown to be the cause of Rett's syndrome (Chao et al., 2007), while genes encoding neuroligins-cell adhesion molecules necessary for linking pre- and postsynaptic terminals are mutated in many autistic patients. The idea that ASDs are affected by the mutations or deletions of synaptic or neuronal activity genes seems very plausible considering the common characteristics of the disorders. A skill loss, for example, could be attributable to the malformation or instability of an existing synapse (Zoghbi 2003). Inability to acquire a language or establish social interactions could stem from difficulty to form new, much more complex connections related to learning and memory that involve synaptic plasticity. The research clearly points to these processes as later events in contrast to the development of the nervous system during prenatal and early postnatal phases that depend on the internal cell programming and activity (Walsh et al., 2008; Zhong, 2003). By the same token, the involvement of distinct genes may manifest the same or strikingly similar phenotype just because they encode proteins participating in the same synaptic process, which appears to be the case in ASDs (Walsh et al., 2008; Zoghbi, 2003). Additionally, plasticity events are very different among individuals resulting from personal experiences, therefore, the onset of symptoms and their extent may very well vary even if the involved synaptic gene is the same. Surely, the malfunctioning

synaptic molecules alone cannot account for the male to female differences in susceptibility to these disorders, which may result from hormonal differences in addition to genes located on the X chromosome. Nevertheless, it is noteworthy that genome wide studies in search for genes related to autism and molecules involved in neuronal activity seem to strongly overlap (Walsh et al., 2008). Recently, the identification of the genes responsible for these disorders and generating animal models becomes increasingly important due to the possibility of gene therapy replacements.

Complex neuropsychological features that characterize ASDs pose difficulties in proper diagnosis of human patients alone, which makes it even harder to recapitulate in animal models. However, many ASD-associated characteristics can be analyzed in mice. For instance, the most striking aspect of social interactions' deficits can be addressed because mice are highly social species (Crawly, 2007). When allowed to interact, they sniff or touch each other, a feature that is quantifiable. In addition, even though, language per se cannot be measured, communication abilities such as vocalizations in pups missing from the nest and their subsequent retrieval by the mothers can be tested. "Autistic" mice may also display repetitive behaviors such as grooming or jumping (Crawly, 2007). Sometimes, autism can be associated with enhanced learning in certain contexts, and this paradox is seen in animal models. For instance, introduction of a mutated form of *Neurologin 3* found in autistic patients into mice results in the impairment of social interactions, but an improvement of spatial learning possibly due to the observed increase of inhibitory transmission (Tabuchi et al., 2007). These findings are interesting as it has been noted that some autistic or ASD patients display significant abilities to memorize things in certain contexts. Often, however, these memories are short lived. As another example, *Shank1* knockout mice show improved spatial learning, but strong deficits in memory retention (Hung et al., 2008).

1.4 Potential roles of IB2 in kinase scaffolding, synapse function, and Phelan McDermid Syndrome

Islet-brain-2 (IB2) also referred to as c-Jun NH2 terminal kinase (JNK) interacting protein 2 (JIP2) is a large cytoplasmic molecule, whose functions have not been clearly elucidated. Its exclusive expression in neuronal and neuroendocrine regions suggests IB2 involvement in neurological processes. Due to its sequence homology to the JIP1/IB1 protein and its weak ability to interact with JNK, IB2 has been classified as a member of JNK interacting protein (JIP) family of scaffolds. Similarly to JIP1, IB2 contains JNK binding domain and Src homology 3 domain (SH3) followed by phosphotyrosine binding domain (PTB) (Negri et al., 2000; Yasuda et al., 1999). As other JIPs, IB2 also possesses motifs called tetratricopeptide repeats (TPRs) that allow for its interaction with the light chain of motor protein kinesin (Verhey et al., 2001). In Rin5F insulinoma cells, IB2 is found concentrated in cytoplasm and colocalized with JIP1 at the tips of neuritic projections, consistent with the finding that JIP1 and IB2 can form heterooligomeric complexes (Yasuda et al., 1999). Expression of the epitope-tagged IB2 in CAD cells along with dominant negative form of kinesin prevents such distribution (Verhey et al, 2001) suggesting that kinesin-IB2 interaction may be necessary for a proper delivery of IB2 in nerve cells. Endogenous localization of IB2 in neuronal cells, however, has not been reported due to the lack of appropriate antibody. Further biochemical analyses employing ectopic coexpression and coimmunoprecipitation have shown that IB2 can self-associate and interacts with a wide array of binding partners. IB2 interacting proteins include among others amyloid β precursor protein (APP), apolipoprotein E2 receptor, and MAPK signaling cascade components similarly to JIP1 (Negri et al., 2000; Stockinger et al., 2000; Yasuda et al., 1999). Unlike JIP1, IB2 also associates with guanine exchange factor TIAM1 (Buchsbaum et al., 2002) and fibroblast growth factors homologous factors (FHF)

as shown in our laboratory (Schoorlemmer and Goldfarb 2001 and 2002). The binding sites for these two proteins on IB2 partially overlap and, as expected, come from an IB2 region that bears no similarity to JIP1. Interestingly, TIAM1 binding to IB2 enhances its interaction with p38 α signal transduction components, whereas FHF association leads to an increase in p38 δ activation in a dose dependent manner. p38s belongs to the mitogen activated protein kinase (MAPK) family along with JNKs and extracellular signal-regulated kinases (ERKs). Each of these MAPKs is activated by specific subset of MAPK kinases (MAPKKs or MKKs) that in turn are activated by MAPKK kinases (MAPKKKs) generating three-gear cascades (Gallo and Johnson, 2002). IB1 (JIP1) binds the MAPKK called MKK7, which phosphorylates JNK, and mixed lineage kinases (MLKs) class of MAPKKKs and is required for stress-induced JNK activation *in vivo* (Whitmarsh et al., 2001; Yasuda et al., 1999). IB2, on the other hand, interacts very weakly with JNK and fails to compensate for the lack of IB1 *in vivo* in this cascade's signaling (Whitmarsh et al., 2001; Yasuda et al., 1999). These findings argue that IB2, if indeed a scaffold, may participate in different MAPK pathways as opposed to JNK signaling cascade. IB2 interacts with p38 α isoform through its JNK binding domain (JBD) and with MKK3 known to phosphorylate p38, and the MAPKKK MLK3, upstream from MKK3. MLK3, in turn, can be turned on by Rac1 GTPase activated by its guanine nucleotide exchange factor TIAM1, which is yet another IB2-interacting protein. The binding of these p38 MAPK cascade components suggests that IB2 may participate in scaffolding of this signal transduction pathway. The involvement of JNK in apoptotic signaling has been well established (Whitmarsh et al., 2001). By contrast, the role of p38 in this process is not very well understood and accumulating evidence suggests its rather broader role in the nervous system cell fate and functioning (Takeda and Ichijio, 2002). Interestingly, p38 MAPK has been recently linked to learning and memory mechanisms

involving LTD and LTP. p38 MAPK is activated in response to NMDAR induction and activation of RasGRF1 that result in LTD in adult mouse hippocampus. This pathway is only activated upon stimulation of NR2B containing NMDARs. NR2B subunits are expressed later in development suggesting the role of this pathway after the initial patterning of the nervous system (Li et al., 2006A). In adolescent mice presented with enriched environment, p38 was shown to be activated in response to NMDAR induction through a cAMP dependent mechanism resulting in LTP at the CA1 hippocampal region (Li et al., 2006B).

Due to the multiplicity of IB2 interactions with the components of different MAPK signal transduction pathways and many other proteins, we considered cellular overexpression or dominant negative approaches unreliable for definitive analysis of IB2 functions. Therefore, in order to elucidate its role *in vivo*, we have generated IB2 knockout mice (Chapter 3). I have shown that IB2 mutant mice display a variety of phenotypes including hypotonia early in development and serious deficits in motor learning and motor performance. In addition, juvenile mutant mice show impairment in social interactions and appear to be unresponsive to novel environments (Chapter 4). The complex IB2 knockout behavioral responses are highly reminiscent of symptoms observed in Phelan-McDermid patients. The human *Ib2* gene is, in fact, situated within chromosome 22q13, only 65kbp away from *Shank3*, a gene deleted in all Phelan-McDermid patients.

My work has further shown that IB2 is an integral component of dendritic postsynaptic densities, a curious similarity to SHANK3 proteins (Chapter 5). Although the molecular composition of PSDs are not grossly altered in IB2 knockout mice (Chapter 5), other supporting work suggests changes in morphology of Purkinje cell dendritic arbors and spines (M.Urbanski, our lab) and altered postsynaptic NMDA currents in cerebellar granule cells (in collaboration with F. Prestori and E. D'Angelo, University of Pavia). These studies have

begun to define critical neuronal functions performed by IB2 and establish *Ib2* mutation as a potential contributor to behavioral deficits found in ASDs and specifically Phelan-McDermid Syndrome.

CHAPTER 2

MATERIALS AND METHODS

RATS and MICE

The rat embryos used for hippocampal and cortical cultures in this study were Sprague Dawley. The mice were generated in our laboratory on the mixed background 129Svev/C57Bl.6 and subsequently backcrossed for 7 generations to 129Svev strain.

DNA and RNA analysis methods:

TAILING, TAGGING AND DNA EXTRACTION

Mice were anesthetized with isoflurane. During anesthesia, an ear tag was attached and a portion of the tail (0.5 inch) was clipped off. Each tail was processed for DNA extraction in 650 μ l of tail lysis buffer (0.05M Tris HCl pH8.0, 0.1 M EDTA, 0.5% SDS) containing 500 μ g/ml of Proteinase K. After overnight incubation at 55°C, tissue debris was removed by centrifugation and DNA extracted with phenol/chloroform. DNA was precipitated with 4M unbuffered NaOAc and 0.1 volume of 100% ethanol. DNA was isolated with sealed-tip Pasteur pipette, washed with 70% and 100% ethanol respectively and dissolved in Tris-EDTA (pH8.0).

SOUTHERN BLOTTING

DNA was digested with EcoRI enzyme and ran overnight at 55V in 0.8% TBE agarose gel for separation. The DNA fragments were transferred from the gel onto the membrane in 0.5N NaOH and prehybridized at 42°C in prehybridization/hybridization solution (50% formamide, 5X SSPE, 2X Denhardt's solution, 8% dextran sulfate and 1% SDS). The IB2 5' radioactive probe corresponding to 700bp fragment cut out with SacI enzyme from IB2

promoter region of a plasmid used to generate a construct (800bp upstream from exon I) was generated using NEBlot kit with 32P-dCTP using 100ng of DNA. The probe was then subjected to purification through the G50 Sephadex column. The conditions for probe hybridization to the fragments on the membrane were the same as prehybridization. Low stringency washes were performed at 68°C for 30minutes with 2x SSC and 0.1% SDS followed by 10 minute high stringency wash 0.1x SSC and 0.1% SDS until desired signal detected by Geiger counter. The sizes of *Ib2* alleles detected by the 5' probe after EcoRI digestion were as follows: 15.7 kb for *Ib2+*, 8.7kb for *Ib2^{flox}* and 5.3 kb for *Ib2-*.

PCR

Four-primer PCR reaction was performed on genomic DNA from mice tails to test for *Ib2*^{+/+}, *Ib2*^{+/-} and *Ib2*^{-/-} genotypes. Two primers used to detect wild type allele (*Ib2*⁺) were: forward-(5'-TCACCAGCGCTCCATGTTGATGCA-3'), backward (5'-TGCCCTGCCTATCTCCATCTTCCT-3') and resulted in 591bp product. The primers used to detect *Ib2*⁻ allele were: forward (GCCTGAAGAACGAGATCAGCAGCCT), backward (CTGGGAGGAGGACATGAGCGTTGA) resulting in 461bp product. The reactions were performed in 50µl volumes (1x cloned PFU buffer, 200µM dNTP mix, 5% DMSO, 50pmol concentrations of each primer, 200ng of tail genomic DNA template and 3U of PFU polymerase from Stratagene). The reaction conditions were: 1 cycle at 96°C for 2 minutes, 5 cycles: 95°C for 1.25 min, 61°C for 2 min and 72°C for 4 min, followed by 25 cycles: 95°C for 1.25 min, 59°C for 2 min and 72°C for 4 min. PCR products were separated on 1.5% agarose gel and visualized with ethidium bromide. Heterozygote DNA (*Ib2*^{+/-}) determined previously by Southern Blotting was used as a positive control for both alleles and distilled H₂O was used in place of a template to serve as a negative control. *Cre* primers were:

forward: gTTCgCAAgAACCTgATggACA and backward: CTAgAgCCTgTTTTgCACgTTC that gives 350bp product.

RT-PCR

Ib2^{+/+} and *Ib2*^{-/-} animals were sacrificed and the brains removed and immediately placed in Trizol reagent and homogenized. Insoluble material was removed by centrifugation at 12000g for 10 minutes at 4°C. Clear supernatant was incubated for 5 minutes at room temperature to permit complete dissociation of nucleoprotein complexes. 0.2 ml of chloroform was added/ 1 ml of Trizol used and contents were thoroughly mixed and incubated at room temperature for 2 minutes. RNA was precipitated with isopropanol at room temperature for 10 minutes followed by centrifugation at 12000g for 10 minutes at 4°C. RNA was washed with 75% ethanol in RNase free water and redissolved in RNase-free DEPC-treated water. 5µg of RNA was used for cDNA synthesis. The synthesis reaction was performed at 42°C for 2 hours in 25µl volume (1x AMV RT buffer, 10mM DTT, 200U Rnasin inhibitor, 0.95 mM oligo-dT primer, 25U AMV Reverse Transcriptase). PCR reaction was conducted with 50ng template DNA and Titanium Taq polymerase from BD Biosciences. The reactions were performed in 50µl volumes (1x Titanium Taq buffer, dNTP, 100pmol primers). The reaction conditions were: 1 cycle at 94°C for 3 minutes, 3 cycles: 94°C for 40seconds, 62°C for 1 min and 72°C for 2 min, 3 cycles: 94°C for 40seconds, 59°C for 1 min and 72°C for 2 min, followed by 25 cycles: 94°C for 40seconds, 56°C for 1 min and 72°C for 2 min. The primers used for *Ib2* gene were as follows: exon I-II (ACCTTTCACTCGCTGTCGCCT and TCACAGTGGTCCGAGTCGTAGC) resulting products size is 134bp, exons III-V (GGAAGAGGAGGAAGATGGAGATAGG and AGGGCGTGCAAGGGACTGTACT) resulting products size is 316bp, exons IX-XI

(TCCTGCCTCTTGTGACCTTGAG and CGGGTGTGGTGGTGAAGC) resulting products size is 168bp, and exons I-XI with 344bp product . For *Ib2* neighboring genes, the PCR conditions were as follows:1 cycle at 94C for 3 min; 3 cycles at 94C for 40sec/60C-1min/72C-2min; 3 cycles 94C-40sec/57C-1min/72C-2min; 25 cycles 94C at 40sec/54C-1min/72C-2min. The primers were as follows for *Shank3*: SHANK3_EX7_F : TGCTCAGAATGCCTCGGGAAAC SHANK3_EX8_B: TGTTGGCACCACGGAAAAGC resulting in a 94bp product; for *Arsa* ARSA_EX9_F: GGTCTTTGCTGTTCGGAATGG ARSA_EX10_B: TTCTGGTAAGGTGGCATCGGAC resulting in 640bp; for *Chkb* CHKB_EX10_F: CACTTTTTCTGGGGTCTGTGGTC and CHKB_EX11_B: AGGATGATGGGGAACTCGTCAG resulting in 135bp product.

Behavioral Assays:

All behavioral assays were performed by the same administrator (myself) at the same time of the light cycle. The equipment used was cleaned between each mouse session in order to avoid olfactory cues.

GRIP STRENGTH

Mouse was tested by placing its forelimbs on the bar and pulling until letting go and the peak force reading was displayed in [N] or [kg] units and analyzed.

INVERTED GRID

An animal was placed in the middle of the metallic grid, which was then inverted by 180° and the time it could hold on to it was being measured for 60 seconds (Wang et al., 2001).

ROTOROD

Animals were first acclimated to the apparatus a day before, two times/day at the following settings (start:1rpm, top:12 rpm, Ramp:179seconds, Total:180s) on a rotorod from IITC Life Science Inc. Mice were then tested for 4 or 5 consecutive days three times/a day with 15 minute intervals between trials at the following settings: Start:1rpm, top :31 rpm, Ramp:360seconds, Total: 360 seconds. The speed in rpm at fall-off was recorded and analyzed for each mouse.

ELEVATED T-MAZE

Animals were tested for conditioned fear (open arm avoidance) and unconditioned (innate) fear (open arm escape) in the elevated T-shaped apparatus composed of one enclosed and two perpendicular open arms that based on innate fear of open spaces in rodents, (Echeverry et al., 2001; Jardim et al., 1999). Before the test, mice were acclimatized in separate cages for 3 minutes and then placed into enclosed arm with removable door closed for 1 minute acquisition (inhibitory avoidance). The door was lifted and the animal allowed to freely explore the T-maze for 5 minutes. During this time, it was videotaped without experiment administrator in the room. The apparatus was cleaned after every mouse to avoid olfactory

cues. The behavior was analyzed as time spent in the enclosed vs. open arm (Echeverry et al., 2001; Jardim et al., 1999). The one way escape (open arm escape) responses were tested in the same manner except for the fact that the mouse at the beginning of the test was placed at the end of an open arm. Both assays were performed on two different cohorts of mice.

SOCIAL INTERACTIONS

Mice participating in social interactions were not siblings. They were singly housed for 5 days prior to the assay and then allowed to interact in a new mouse cage for 10 minutes. Their interaction was videotaped without an administrator in the room. The time mutant or wild type pairs spent interacting e.i. sniffing and touching was recorded.

NOVEL OBJECT RECOGNITION

The test was performed in a black box (75cmx75cm) with the 2 objects placed at the equal distance from the opposite corners. Each tested mouse was exposed for 15 minutes to the two objects for two consecutive days. On the third day, after 5 minutes, one of the objects was replaced by a bigger and coloristically distinct object and a mouse was allowed to explore it for the next 10 minutes. The number of approaches to each object was recorded and analyzed.

OPEN FIELD

In the open field test a mouse was placed in a center of the transparent guinea pig cage for 30 minutes and videotaped alone in the room. The time each mouse spent in the center vs. time spent at the edges of the cage was recorded and analyzed. The cage was cleaned with water between each mouse use in order to avoid olfactory cues.

DARK-AND-LIGHT PARADIGM

The black box (75cmx75cm) was equally divided into two compartments. Half of it was brightly illuminated and the other was covered in order to create the dark compartment. Both areas were separated by the small entrance to the dark portion of the box. A mouse was placed in a bright area in front of the entrance facing the opposite direction.

Cell Culture Methods (Cortical and Hippocampal):

Pregnant rat or mouse females from *Ib2* heterozygote matings were sacrificed with CO₂ in order to obtain E18 embryos. Tails were saved for DNA extraction and genotyping purposes and hippocampi (and cortices for the cortical cultures) were quickly dissected out and processed separately. They were digested with papain and cells were grown in multiwell plates on 12 mm diameter coverslips coated with poly-D-lysine (20µg/ml) and laminin (3µg/ml) at 50,000 cells/coverslip for signal transduction analyses and subsequent protein extractions (or 30,000 cells/coverslip grown upside down for immunofluorescence) of a 24-well plate in Neurobasal/B27 medium (Gibco BRL), supplemented with glutamine, and

penicillin/streptomycin. Neurons were re-fed with final concentration of 2 μ M cytosine/arabinoside/deoxycytidine every three days in culture in order to destroy dividing cells. In hippocampal cell culture, glia conditioned media was included and partial media change was performed every three days (Tollias et al., 2005).

CELL DNA EXTRACTION

Plates were chilled on ice and the media was aspirated, followed by addition of buffer containing 100mM Tris (pH8.5), 5mM EDTA (pH8.0), 0.2%SDS, 200nM NaCl and 100 μ g/ml of proteinase K and placed at 37°C overnight. Equal volume of isopropanol was added and plates were rocked for 1 hour at room temperature. DNA was removed using Pasteur pipette, washed in 70% and 100% EtOH and placed in 1x TE buffer (10mM Tris pH7.5 and 1mM EDTA pH8.0) at 37C overnight.

CELL CULTURE OR BRAIN PROTEIN EXTRACTS

Triton protein lysis buffer was added to each well with primary cell cultures (or brains) (Triton lysis buffer: 20mM Tris pH7.4, 137mM NaCl, 2mM EDTA, 25mM beta-glycerophosphate, 2mM Na pyrophosphate, 1mM Na Orthovanadate, 10% glycerol, 1% triton, 1mM PMSF, 10 μ g/ml aprotinin, 10 μ g/ml leupeptin freshly added). In case of cultures cells were scraped off, transferred to tubes and allowed to sit on ice for 10 minutes. Subsequently, cell or brain extracts were vortexed and spun down for 10 minutes at 13,000rpm at 4°C. Supernatants were stored at -80°C.

CELL FIXATION AND IMMUNOFLUORESCENCE

Cells were fixed for 20 minutes with pre-warmed 4% PFA/4% sucrose at room temperature on the coverslips positioned upside down. Subsequently they were permeabilized for 10 minutes with 1% Triton in 1xPBS. Then, they were blocked for 1 hour in 20% serum in PBT buffer. Primary antibodies were applied overnight at 4°C at 1µg/ml in PBT with 2.5% BSA. The secondary antibodies were applied at 1:100 dilution for 1 hour at room temperature. The following antibodies were used: anti-IB2 (Antibodies Inc.), anti-tubulin-FITC (Sigma), phalloidin-rodamine and phalloidin-Cy5 (Invitrogen), goat anti-mouse Cy5 (Millipore), and goat-anti-mouse-Alexa488 (Invitrogen).

BRAIN FRACTIONATION

The cortices were dissected out from wild type and mutant mice and homogenized (0.32M sucrose, 0.1mM CaCl₂, 1mM MgCl₂, 0.1mM PMSF, 25mM NaF, 1mM Na₃VO₄). CaCl₂ was added to 1.25M and part of this solution was stored as fraction 1. The remaining amount was placed in the ultracentrifuge tubes with 1.25M:1M:0.32M sucrose solutions and centrifuged for 3 hours at 100,000g at 4°C. Synaptosomes (fraction 2) were collected from 1.25M interface with a needle. A portion of fraction 2 was diluted and solubilized with 1% Triton, rotating at 4°C for 30 minutes, and then centrifuged for 30 minutes at 40,000g. The resuspended high-speed pellet constituted the postsynaptic density fraction (fraction 4).

IMMUNOPRECIPITATION

1 μ g of anti-IB2 antibody was added to 3mg of proteins in 1% Triton lysis buffer and incubated for 36 hrs on ice. The next day protein G-sepharose beads were rinsed off, resuspended in Triton lysis buffer, added to the immunoprecipitates and tubes were rotated for 30 minutes at 4°C. Beads were then collected by centrifugation, and washed twice with Triton Lysis buffer. Sample buffer (2% SDS – 125 mM Tris pH6.9 – 70 mM beta-mercapthoethanol – 0.025% bromophenol blue) was added and beads were boiled for 5 minutes. The boiled-off supernatants extracted from beads were subjected to Western Blot analysis.

WESTERN BLOTTING

The samples were loaded onto 10% polyacrylamide SDS gels and subjected to electrophoresis overnight at 75mV in a running buffer (Tris-Glycine buffer, 0.1% SDS and 10 mM β -mercapthoethanol). The next day, the gel was transferred for 3 hours at 800mA onto PVDF membrane (Millipore) previously wetted in methanol. After transfer, the membrane was blocked with 5% milk in TBS for 1.5 hours at room temperature. The primary antibody incubation was performed overnight at 4C with rocking in 2.5% BSA in TBS. Secondary antibody incubation was done at room temperature for 1.5 hours. The membranes were developed in ECL reagent (Amersham).

GOLGI STAINING

Mice were anaesthetized with acepromizine and ketamine injected intraperitoneally. Subsequently, they were immobilized and 1xPBS with heparin was injected into left ventricle. At that moment right atrium was cut and PBS was being pumped slowly into ventricle. After pumping of PBS the syringe was switched to 4%PFA in 0.1M phosphate buffer with 1.5% picric acid. 20ml of fixative was injected. Then, brains were removed and sliced in vibratome bath filled with 3% potassium dichromate. The slices were incubated overnight at room temperature in potassium dichromate. They were then placed on slides and covered with coverslips in 1.5% silver nitrate solution for 1-3 days covered with aluminium foil. Slices were then washed with ethanol and xylene and fixed on the slides with Permount.

CHAPTER 3
GENERATION OF IB2 KNOCKOUT MICE

Introduction

IB2 is a putative scaffold protein, discovered on the basis of sequence homology to Jnk interacting protein 1 (JIP1) or IB1 (Negri et al., 2000; Yasuda et al., 1999). Both molecules possess JNK binding domain (JBD), Src homology 3 domain (SH3), phosphotyrosine binding domain (PTB) and motifs for interaction with motor protein kinesin. Additionally, they share multiple binding partners and can form homo- and hetero-oligomeric complexes (Verhey et al., 2001; Yasuda et al., 1999). However, closer biochemical examination implicates different signaling module assemblies on these scaffold proteins and distinct binding partners (Buchsbaum et al., 2002). Furthermore, *Ib1* wide expression is not paralleled by *Ib2*, which is limited to neuronal and neuroendocrine regions. Finally, IB2 fails to compensate for the lack of IB1 in JIP1 knockout mice. These findings suggest distinct roles for these two molecules. IB1 serves as a scaffold for JNK pathway components whereas IB2 may aid in p38 mitogen activated protein kinase (MAPK) signal transduction.

The complexity of IB2 interactions as well as controversial speculations regarding scaffold functioning tightly connected to its concentration makes genetic approaches such as overexpression or dominant negative methods unsuitable to study its function (Ferrel, 2000). Therefore, our laboratory chose to investigate IB2 role through gene targeting. Prior to initiation of my research, genetically engineered mice containing *Ib2* floxed (containing loxP sites) allele were generated (Bhandhyopadhyay and Goldfarb, unpublished data) (Fig.3-1).

Results

This chapter will describe the generation of *Ib2* conditional knockout mice with the strong emphasis on the need for and creation of the full *Ib2* knockout animals. Subsequent necessary breeding strategies and genotyping methods will also be discussed.

Last, the proper gene expression within *Ib2* genomic context in the mutant will be demonstrated indicating these knockout mice as suitable model for investigating the neurological function of IB2 molecule.

Generation of *Ib2* conditional knockout mice

Mice with the genetically engineered *Ib2* allele were previously generated in our laboratory. This modified allele contains lox P sites flanking exons III-VIII (Fig.3-1). These major exons in *Ib2* gene encode the portion of the IB2 molecule that encompasses JBD, SH3, PTB and the middle region that are necessary for nearly all interactions with its binding partners such as FHF_s, p38 MAPKs α and δ , their upstream activators MKKs and MLKs, and TIAM1 (Schoorlemmer and Goldfarb, 2002).

In order to generate conditional knockout mice, the heterozygotes containing wild type and floxed allele were bred with mice expressing *Cre* recombinase under the *CamkII α* promoter generously provided by Dr. Scott Zeitlin (Dragatsis and Zeitlin, 2000). CAMKII α is a calcium/calmodulin dependent kinase highly abundant in the brain with the forebrain being its predominant expression site. Resulting offspring would possess the wild type, modified and the knockout allele only in the brain of those that also express *Cre* recombinase. Assuming that *Ib2* gene dosage is not crucial, a possible lethal phenotype could

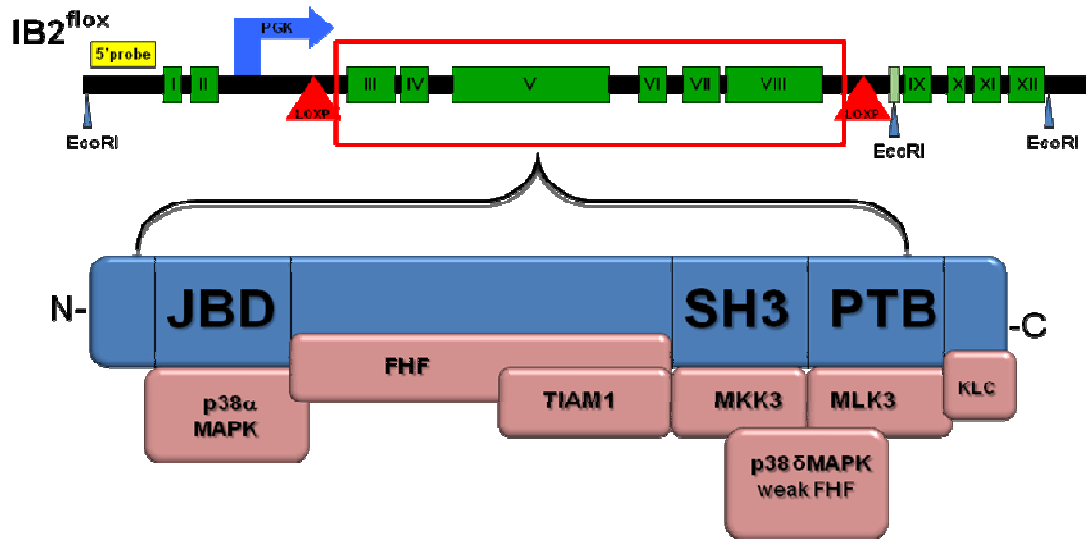


Fig.3-1

Schematic illustration of the modified mouse *Ib2* allele and IB2 protein. Green boxes represent coding exons. In the modified allele coding exons III-VIII are surrounded by LoxP sites and can be deleted by CRE recombinase. This region of the gene encodes nearly entire portion of IB2 protein (JBD, SH3 and a portion of PTB domain along with intervening portion) necessary for its interactions with the binding partners represented below (p38MAPK α and δ , FHF, TIAM1, MLK3 and MKK3).

be avoided with such genetic composition and these animals could be used as conditional knockout colony founders. The genotyping of the progeny that came from these matings was performed to detect the presence of the CRE transgene and to analyze the *Ib2* alleles. For CRE screening DNA was simply extracted from the tip of the mouse tail and subjected to polymerase chain reaction (PCR) using primers from CRE gene (Fig.3-2). To genetically examine *Ib2* allele composition, DNA was extracted from the brain where the CRE was expected to be expressed and from the liver and kidney to serve as negative control and subjected to Southern Blotting analysis. For this purpose, DNA was digested with EcoRI restriction enzyme. *Ib2* wild type allele possesses two recognition sites for this enzyme: first within its promoter region and the second following exon XII, resulting in 15.7kb DNA fragment upon digestion. The modified allele has an extra EcoRI digestion site within the second loxP region generating the 8.7kb and 5.3kb sequence for the floxed and a deleted allele respectively. The radiolabeled 5' probe recognizing promoter region following the first restriction site hybridizes to all three alleles. As predicted, in animals expressing *Cre*, mutant allele was present in the brain in addition to the wild type and floxed one also found in liver and kidney. The presence of the floxed allele in brain sample of these mice can be explained by the lack of *CamkII* expression in glia and epithelial cells. Therefore, in order to test recombination efficiency specifically in neurons, the homozygote mice (*IB2flox/flox/Cre+*) were allowed to mate and the cortical neuron cultures were prepared from E18 embryos processed separately. After two weeks in culture (DIV14), DNA was extracted from cells and analyzed. The presence of *Cre* was tested by PCR (data not shown) and the recombination efficiency by Southern Blotting. It turned out that the cells prepared from different embryos all positive for *Cre* transgene, demonstrated full recombination efficiency of the floxed allele in some and incomplete one in others (Fig.3-4). It can be speculated that differences in the

effectiveness of CRE mediated deletion lie in haploinsufficiency of *Cre* gene. Alternatively, it could be a stochastic process. The *Cre* integration site in mice provided by Dr. Zeitlin's laboratory was unknown, therefore an effort to indicate this DNA region to allow for simple PCR screening of *Cre* homo- and heterozygotes was undertaken (data not shown).

Meanwhile, the viability and the lack of severe abnormalities in *Cre*⁺ animals born from *IB2flox/flox/Cre*⁺ intercrosses suggested that IB2 related deficits might be more subtle. The predicted analysis would have to require a wide array of behavioral, cellular and molecular approaches. With respect to behavioral assays, they would have to be performed using randomly chosen animals with their genotype and CRE deletion efficiency determined postmortem. If the recombination efficiency would in fact turn out to be random, it would be necessary to generate large animal cohorts to be tested and the percentage of true conditional knockout offspring could not be determined. The conditional knockout approach under these circumstances appeared to be extremely inefficient and time consuming; therefore, any efforts to determine the *Cre* integration site that would enable us to screen for *Cre*^{+/+} mice, were superseded by the decision to generate full knockout mice utilizing CRE recombinase system.

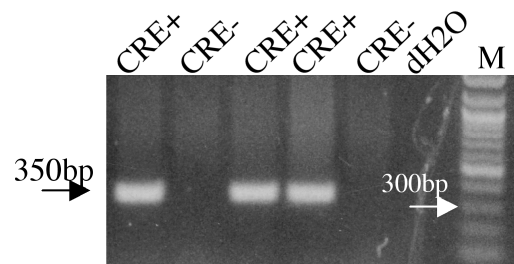


Fig.3-2

PCR reaction testing for the presence of *Cre* gene. Lanes 1,3,4 represent desired progeny that contains *Cre* gene whereas lanes 2 and 5 represent *Cre*- offspring.

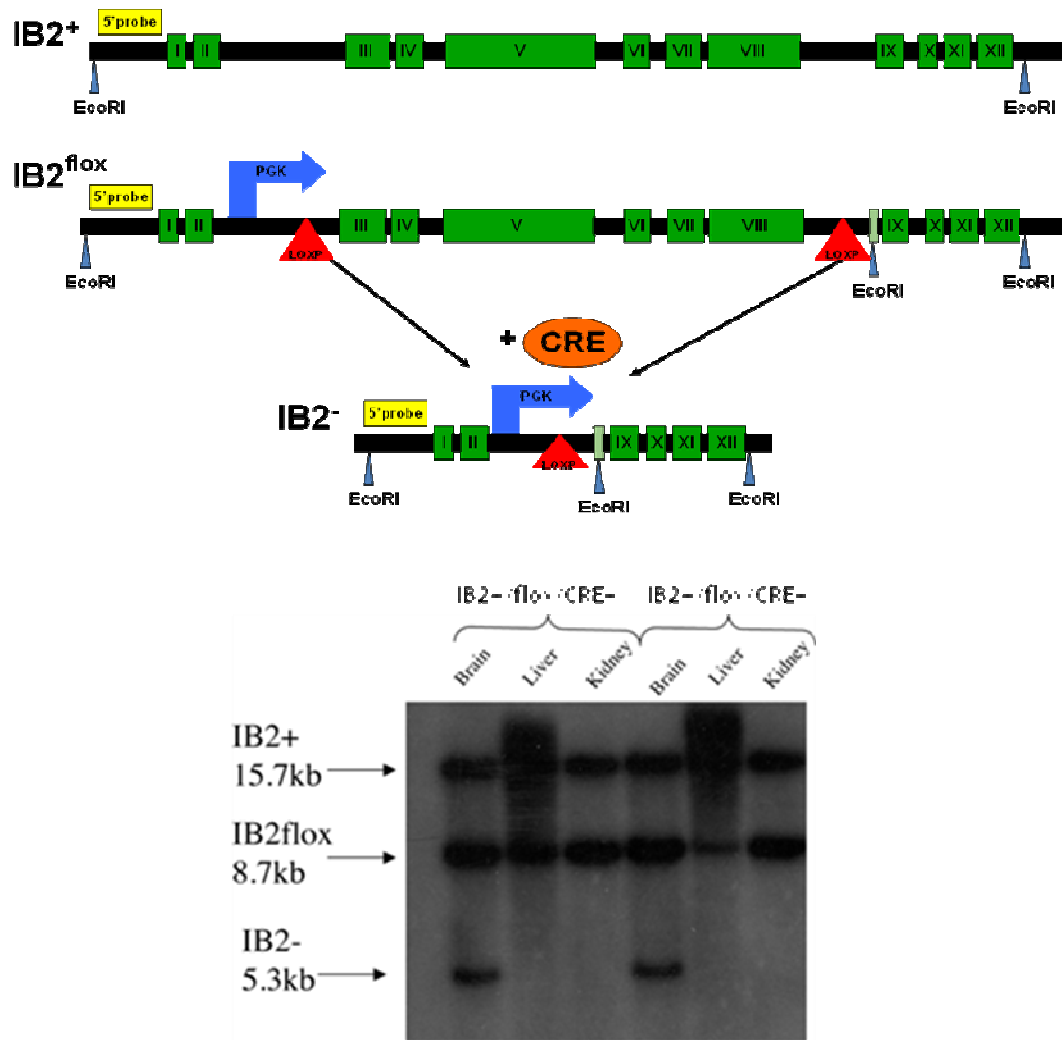


Fig.3-3

Southern Blotting analysis of the heterozygote mice containing *Ib2* wild type and modified allele and expressing *Cre* recombinase determined by the PCR. DNA was extracted from the brain as well as liver and kidney for control purposes. Above is an example of two separate animals. As expected the knockout allele is absent from the liver and kidney. The presence of three alleles: wild type, floxed and deleted was found in the brain. It could be a reflection of other cells in the brain such as a glia, which do not express the *CamkII* and/or the low recombination efficiency.

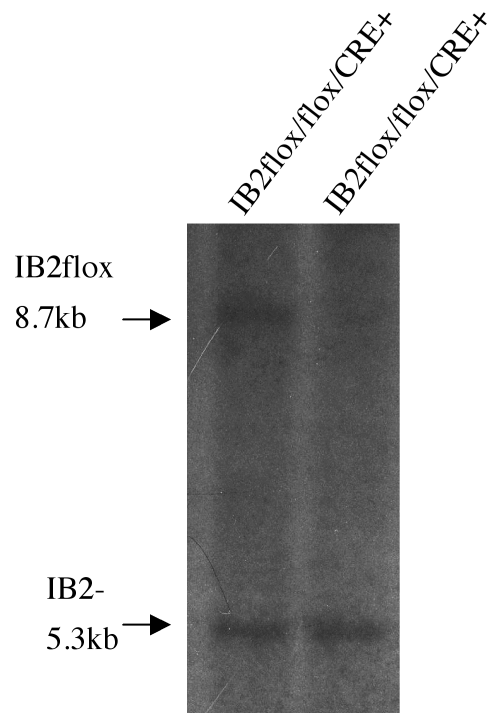


Fig.3-4

Southern Blotting analysis of the cortical cell cultures DNA derived from the *IB2flox/floxCre+* embryos. Two lanes correspond to the cells from two different embryos. The first lane shows both floxed and deleted allele whereas the other one only a knockout one.

Generation of *Ib2* full knockout mice

In order to generate full knockout mice we took advantage of our existing animals with the *Ib2* floxed allele and *Cre* recombinase system to remove the gene by microinjecting *Cre* on a plasmid DNA into fertilized eggs. To prevent the possibility of lethality in a full *Ib2* knockout, wild type females (129Svev strain) were mated with the *IB2^{flox/flox}Cre* (C57Black6/129Svev mixed background) males to generate heterozygote embryos (*Ib2^{+/flox}*). To prepare for microinjection of the DNA specifically into pronuclei before fusion, the wild type females were subjected to the specific hormone regimen geared towards increasing their fertility and specifically time their ovulation. First, they were given a pregnant mare's serum gonadotropin (PMSG) injection, which stimulates the development of ovarian follicle in a manner similar to follicle stimulating hormone (FSH). It was followed forty eight hours later by human chorionic gonadotropin (hCG), which acts as the luteinizing hormone. The matings were set up late in the afternoon to allow for the morning collection of fertilized eggs at one cell stage. The eggs were removed from females and transported at room temperature to the Mount Sinai School of Medicine where they were injected *Cre* plasmid DNA by Dr. Kevin Kelley at the Mouse ES/Transgenic Shared Resource Facility. Following microinjection into male pronuclei, eggs were implanted into surrogate mothers provided by the facility.

The *Ib2* genetic composition of progeny derived from these manipulations was assessed by Southern Blotting. The resulting offspring were: chimeras that possessed three alleles *Ib2^{+/Ib2^{flox}/Ib2⁻}* where the incomplete CRE mediated recombination took place or the deletion occurred following cell division, heterozygotes *Ib2^{+/Ib2^{flox}}* where the process of recombination failed, and finally the desired progeny that were heterozygotes for wild type

and knockout allele (*Ib2*^{+/Ib2-}) (Fig.3-5). *Ib2*^{+/-} heterozygotes were chosen to mate in order to generate the full *Ib2* knockout mice. The mutant animals were born with the expected Mendelian ratios of ~25% indicating no embryonic lethality.

Necessary breeding strategies and genotyping methods

In order to generate *Ib2* knockout mice, the mutant mice were allowed to mate. The progeny born from these intercrosses were viable and fertile. However, their breeding efficiency was very poor, which could have been a reflection of underlying neurological deficits of these animals (CHAPTER 4). Therefore, the heterozygote matings became a standard method for generating mutant progeny. For subsequent studies, some mice were analyzed on the mixed 129Svev/C57Bl.6 background. Additionally, backcrosses to the 129Svev strain were undertaken to obtain purer genetic background.

Offspring born to heterozygote parents were weaned at postnatal day 21 and their tail DNA was used for genotyping. For convenience and necessity for quick genotyping of heterozygote derived progeny, a four primer PCR reaction where wild type and mutant allele are simultaneously recognized was designed and optimized (Fig.3-6). These matings and genotyping strategy became a standard method for generating and choosing mice for analytical experiments aiming at elucidation of IB2 function.

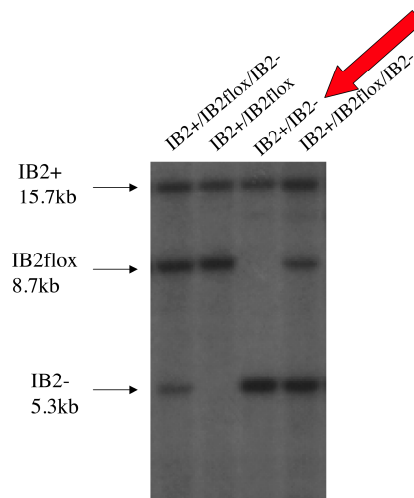


Fig.3-5

Southern Blotting analysis of the progeny following *Cre* microinjection into fertilized eggs. Three types of animals were generated: chimeras with triple alleles- wild type, floxed and the knockout one (lane1 and 4), heterozygotes for wild type and floxed allele where the recombination was unsuccessful (lane 2) and the desired progeny that had the wild type and knockout allele (lane 3). *Ib2+/Ib2flox* mice were chosen to breed to generate full knockout mice colony.

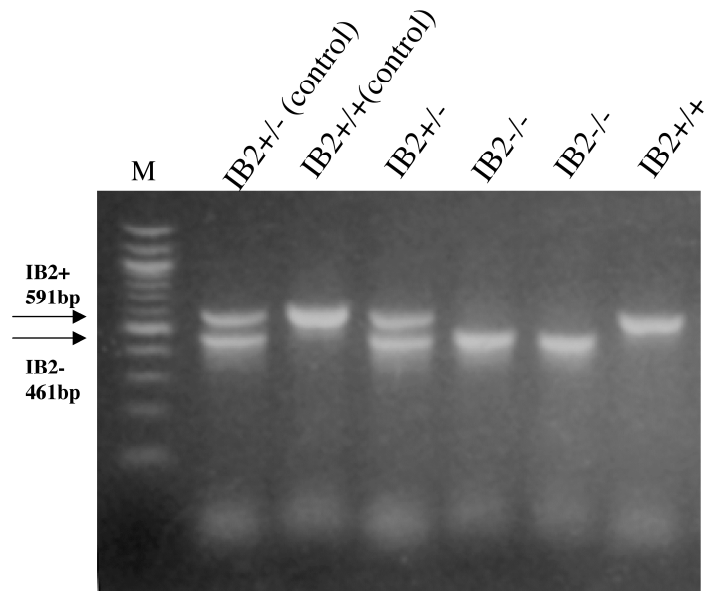


Fig.3-6

The four primer PCR reaction used to genotype the progeny from heterozygote matings. A pair of primers that recognizes the wild type *Ib2* allele (*Ib2+*) generates 591bp fragment whereas the pair that recognized a deleted allele results in 461bp product. Lanes 2 and 4 show heterozygote animals (*Ib2+/-*). Lanes 3 and 7 indicate wild type progeny and the lanes 5 and 6 represent mutant animals.

Assesment of the remaining Ib2 fragment expression in Ib2 knockout mice

The successful removal of loxP flanked DNA in newly generated *Ib2* knockout mice, was determined by Southern Blotting and PCR analysis. However, the engineered animals still contained PGK promoter and remainders of *Ib2* gene, which could be expressed and affect the proper functioning of the neighboring genes. This possibility was tested by RT-PCR. Briefly, RNA was removed from the wild type and mutant brains, treated with the DNAase to avoid genomic DNA contamination and cDNA library was generated using reverse transcriptase. The subsequent PCR step was performed using primers from the regions outside and inside loxP sites. As expected, the primers from exons III and V missing in the knockout generated the product only in a wild type sample (Fig.3-7a). The region preceding and following loxP site are left intact in the mutants and as it turns out both are expressed (Fig.3-7a, Fig.3-7b). The fragment preceding the first loxP site encodes the short N-terminal sequence, which has not been implicated in any IB2 protein-protein interactions. The *Ib2* exons following the second loxP site, on the other hand, encode the TPR motifs necessary for binding to the motor protein kinesin. We wondered whether these sequences are spliced out together in a mutant to generate one fragment. Using primers from exons I (forward) and XI (backward) indeed resulted in a product of expected size in a knockout absent from the wild type (Fig.3-7b). However, we do not expect that this could affect our IB2 related analysis of the knockout mice as this expression would result in a highly truncated polypeptide with little or potentially no functionality nor stability.

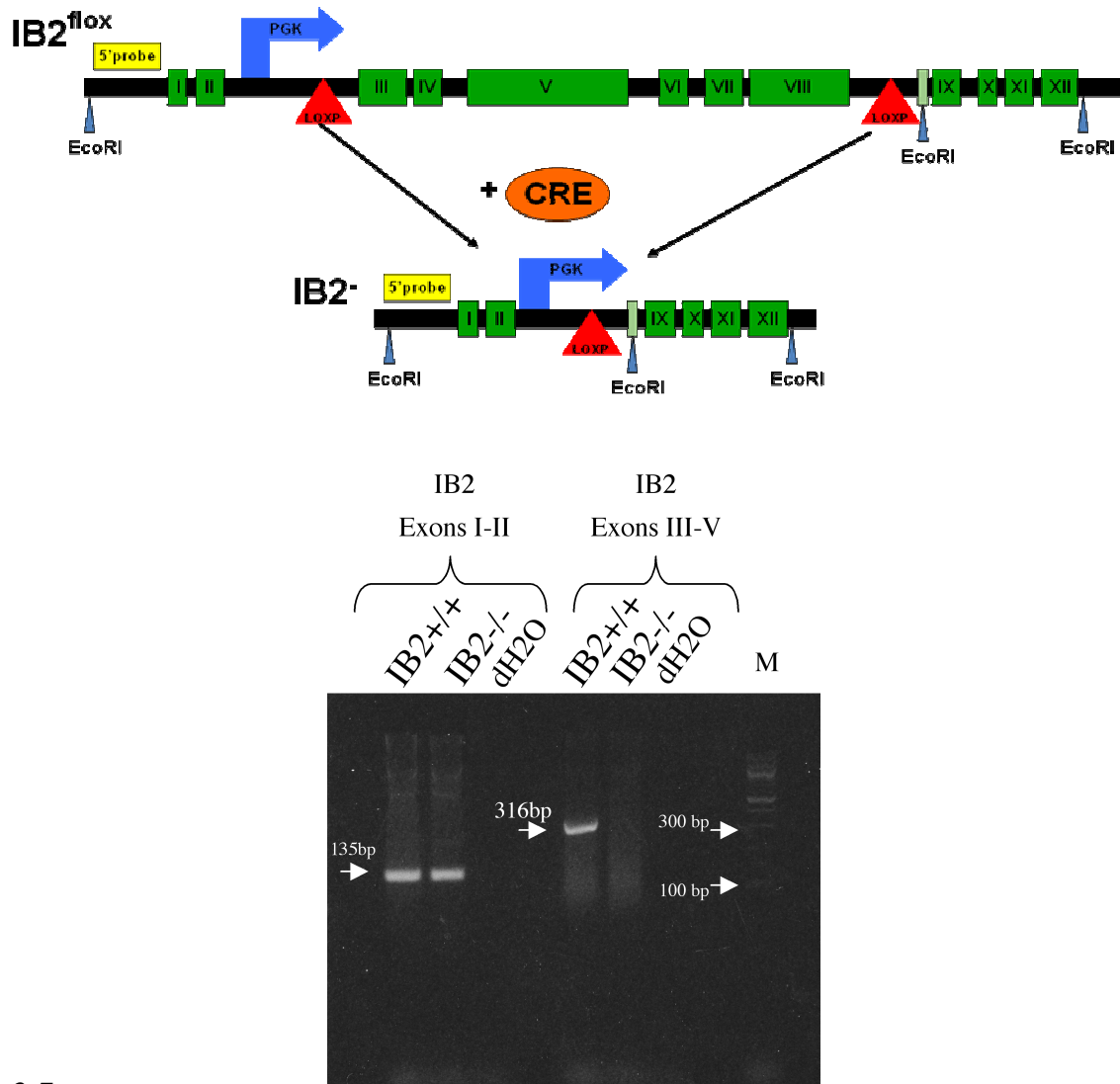


Fig.3-7a

RT-PCR analysis of *Ib2* expression in wild type and mutant mice. Two sets of primers were used: first pair corresponds to the exons I and II that precede the loxP site and from exons III and V that lie within loxP region. As expected the exons I and II are expressed in both wild type and knockout mice whereas region surrounded by loxP sites is missing in the mutant mice. Water was used as a negative control.

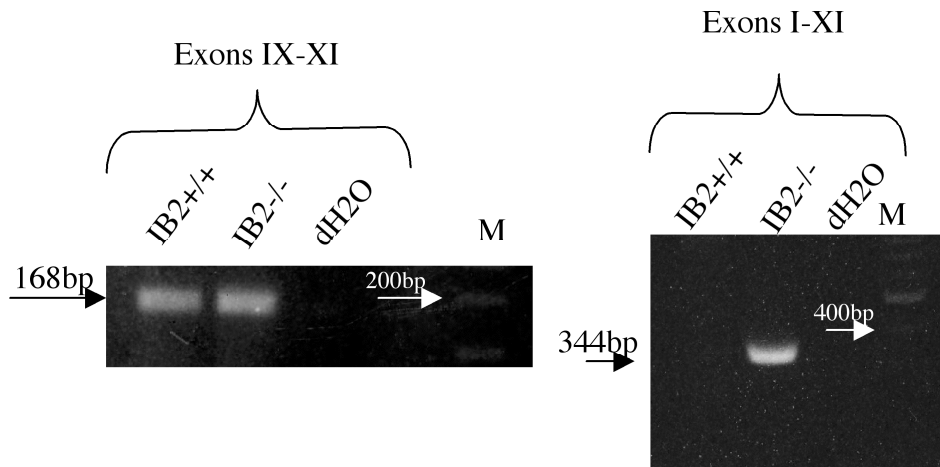


Fig.3-7b

RT-PCR analysis. The primers from the region following loxP sites (exons IX-XI) and the exons I and XI revealed the expression of the C-terminal sequence (left) as well as a spliced out form containing fragment of the N and C-terminal regions in *Ib2* knockout animals (right).

Ib2 knockout does not alter expression of neighboring genes

As previously mentioned the PGK promoter in the construct region preceding the first loxP site is left intact in the mutant mice. This PGK promoter or the deletion of *Ib2* genomic sequences could, hypothetically, affect the expression of the neighboring genes. In such case, the phenotype observed in the knockout could reflect a function of a protein encoded by a gene different from *Ib2* or their synergistic effect. Therefore, we decided to closely examine genomic organization and expression surrounding the *Ib2* locus. *IB2* is located on a murine chromosome 15 at the location 15E3. Its neighboring genes are choline kinase beta (*Chkb*), arylsulfatase A (*Arsa*) that are transcribed in the opposite direction and, further downstream, SH3/ankyrin domain gene3 (*Shank3*) (Fig.3-8). *Chkb* encodes the enzyme-choline kinase that phosphorylates choline/ethanolamine. The lack of *CHKB* in a mouse is manifested by bone deformity and hindlimb muscular dystrophy (Wu et al., 2009). *Arsa* encodes Arylsulfatase A, an enzyme localized to lysosomes and responsible for breaking down sphingolipids, which are the major components of myelin. The lack of this enzyme results in accumulation of sulfatides and leads to metachromatic leukodystrophy (MLD) in humans. In the mice missing this gene, the disease is much less severe. At one year of age they seem to have impaired gait and motor coordination and display hyperactivity (Sevin et al., 2007). *Shank3* encodes SH3 and multiple ankyrin repeat domains 3 protein. *SHANK3* is a scaffold protein with SH3 domain, a PDZ domain, a long proline-rich region, and a SAM domain to interact with its multiple binding partners. In neuronal cells during development it concentrates in growth cones of axons and dendrites and in more mature system it localizes to postsynaptic density region (Sheng et al., 2000). It is hypothesized that through its protein-protein interactions it scaffolds metabotropic and ionotropic components at the excitatory synapse. Its location

further inside the cytoplasm and ability to interact with actin regulatory components indicates its role as a synapse organizer (Sheng et al., 2000). Unfortunately, the *Shank3* knockout mouse has not yet been described. In humans, point mutations in *Shank3* gene have been found in autistic patients. Additionally, it has been implicated in a disease referred to as a 22q13 Deletion or Phelan-McDermid Syndrome. The disorder is manifested by complex phenotype, similar to the one observed in autism spectrum disorders. One of its interesting features is that a skill acquired by the individual is lost several weeks later possibly due to synaptic instability (Wilson et al., 2003). The fact that the particular symptoms differ from patient to patient and the size of the deletion varies suggests participation of additional genes in this syndrome. *Ib2* close localization to *Shank3* and deletion in nearly all affected individuals along with its exclusive expression in the nervous system makes it a very likely candidate involved in this disorder.

Due to the above reasons, the expression of *Ib2* neighboring genes was tested using appropriate primer pairs and cDNA from the wild type and *Ib2* knockout mice brains. As shown in Figure 3-7, the expression of *Chkb*, *Arsa* and *Shank3* is unaffected in the mutant. Therefore, any deficits found in *Ib2* knockout mice will be attributable to the lack of functional IB2 protein.

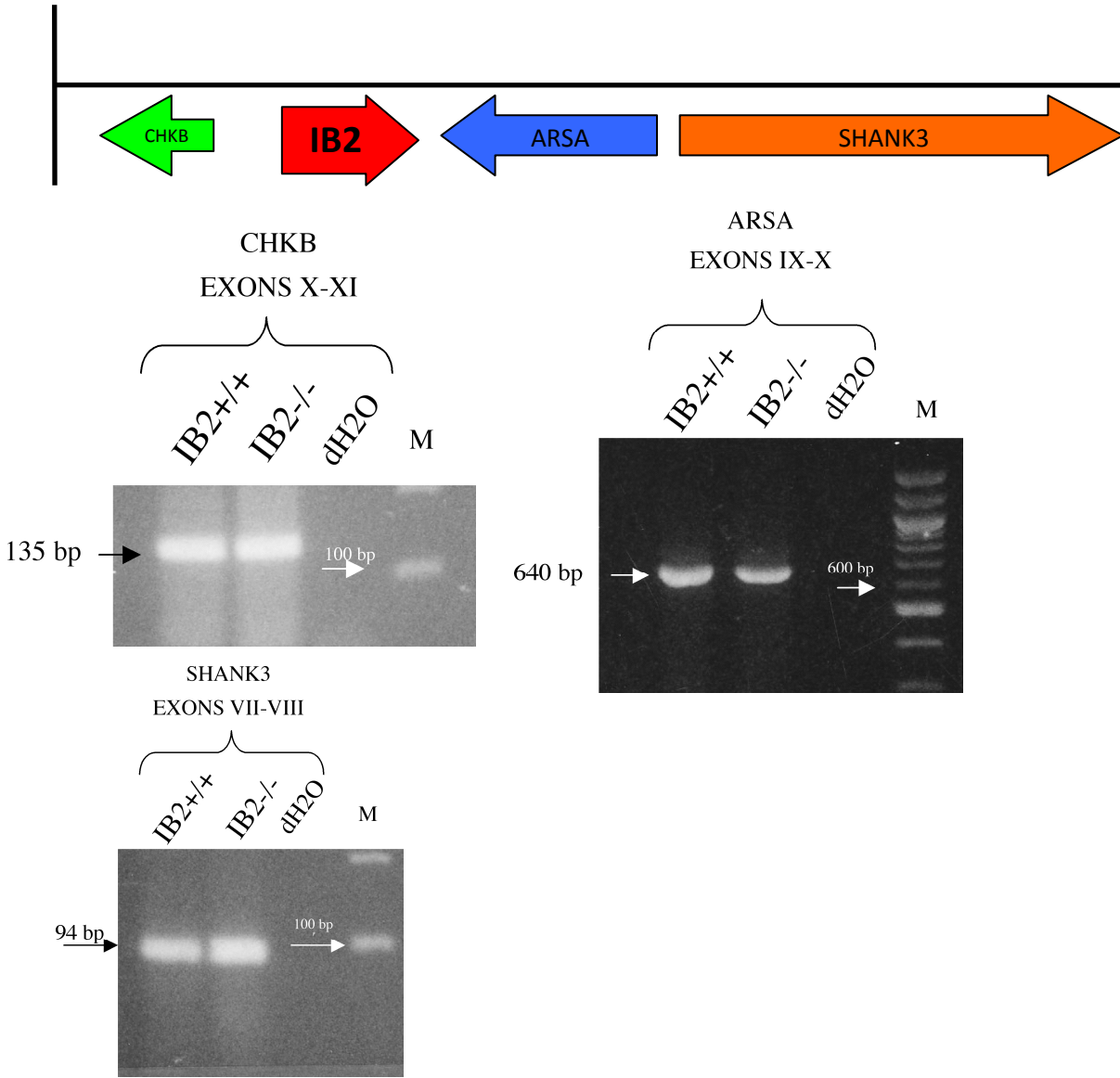
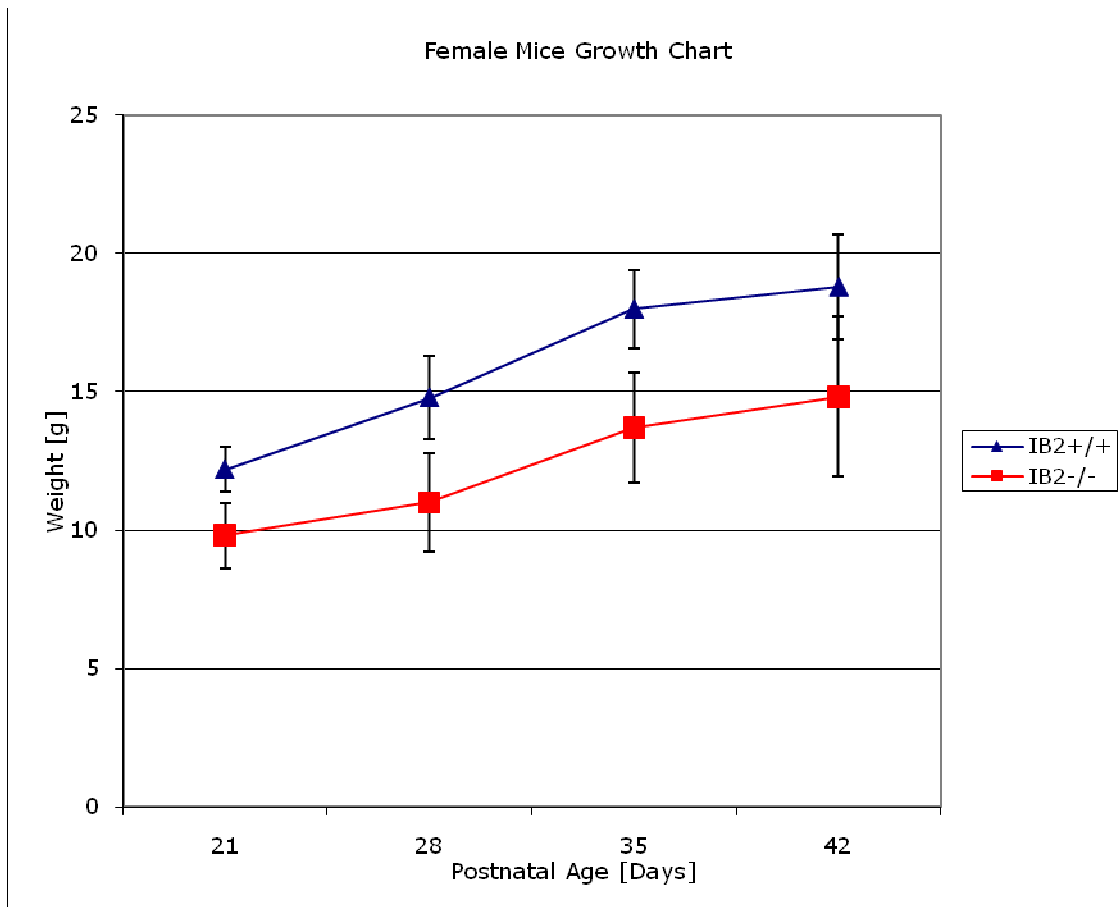


Fig.3-8

Ib2 is localized on murine chromosome 15 at the location 15 E3 between *Chkb* and *Arsa* genes and downstream from it lays *Shank3* gene. The expression of its neighboring genes was tested by RT-PCR. The primers were chosen from exons corresponding to the particular genes. As seen above, all of them are expressed in both wild type and the knockout mouse brains.

Discussion

The complexity of IB2 interactions led us to use the reverse genetics approach in order to establish the function of this putative scaffold protein. The generation of the *Ib2* conditional knockout and the lack of lethal or severe phenotype along with difficulties in genotyping methods and various degrees of CRE mediated recombination posed enormous difficulties in generating mutant animals suitable for analysis of IB2 function and led us to generation of *Ib2* full knockout mice. These animals are viable and appear normal to the first approximation. The only observed abnormalities are the poor breeding performance, which brings upon a necessity of heterozygote matings to generate the knockout mice and the 20% growth deficits observed in mutant mice (Fig.3-8). The lack of visible and severe physical impairments allows us to conduct the broad spectrum of behavioral, cellular and molecular assays in quest for IB2 neurological function.



Age[Days]	IB2-/- N=6 Average [g]	IB2-/- St Dev	IB2+/+ N=5 Average [g]	IB2+/+ St Dev	Student's T test
21	9.8	1.2	12.2	0.8	p<0.004
28	11.0	1.8	14.8	1.5	p<0.004
35	13.7	2.0	18.0	1.4	p<0.003
42	14.8	2.9	18.8	1.9	p<0.03

Fig.3-9

The growth chart of *Ib2* mutant and wild type mice (129 Svej background). The analysis was performed from the day animals were weaned (P21) and every week thereafter until P42, indicating persisting weight deficits.

CHAPTER 4

BEHAVIORAL ANALYSIS OF IB2 KNOCKOUT MICE

Introduction

IB2 is a putative scaffold protein for JNK and/or p38 MAPK signaling, but its exact role has not been elucidated. In humans, the *Ib2* gene is located on chromosome 22 to which several neural diseases have been mapped (Negri et al., 2000). For instance, in Phelan-McDermid syndrome also called 22q13 Deletion, a portion of chromosome in a region 13 is missing (Wilson et al., 2003). Common features found in children with this chromosomal abnormality are hypotonia, sleep disorders, impaired early responses to the environment, affected sensory processing and motor skills, language and communication deficits (Philippe et al., 2008). Being a very close neighbor to *Shank3* gene, implicated in this syndrome, *Ib2* is also missing in all but one analyzed patients (Wilson et al., 2003), which makes it a very likely candidate contributing to this disorder. In addition, IB2 is expressed exclusively in neuronal and neuroendocrine regions, which strongly suggests its neurological function. Its expression within the nervous system is ubiquitous with the highest levels found in cerebellum, pituitary gland, occipital lobe and amygdala (Negri et al, 2000). Cerebellum is mainly responsible for fine movement coordination and motor learning. Pituitary gland is involved in production of growth and sex hormones. Occipital lobe receives and processes sensory information from retina. Amygdala, on the other hand, participates in emotional learning and fear responses. Due to the complexity of described IB2 interactions, its broad neuronal expression and variety of phenotypes in 22q13 deletion, we decided to perform a broad behavioral survey of IB2 knockout mice.

Results

This chapter will present results of behavioral assays conducted on *Ib2* knockout vs. wild-type mice, focusing on tests that showed deficits in IB2 mutant mice. All experiments compared wild-type and mutant mice on the same 129Svev/C57Bl6 mixed strain background or purer 129Svev backcrossed for 7 generations. The similarities of IB2 knockout phenotype to Phelan-McDermid Syndrome will be discussed.

Ib2 mutation causes developmental delay in Grip strength

In order to begin the behavioral analysis of IB2 mutant mice, the classical tests for functional neurological deficits were employed. One such commonly used assay is so called “Sensorimotor Battery”. It consists of four tests: platform, ledge, walking initiation and inverted screen, designed to qualitatively assess balance, coordination, muscle strength and movement initiation (Wang et al., 2002; Wozniak et al., 1996). In all four, an animal is subjected to 60 seconds of analysis during which it is simply placed on a small platform, thin ledge, inside an outlined square or on the grid respectively and the amount of time it can remain there is being recorded.

No differences were found in the platform, ledge and the walking initiation assays (data not shown) in animals that were weaned from the parents at the postnatal day P21-P23 indicating no gross motor skills impairment. However, the deficits were observed in the inverted grid assay (Fig.4-1). IB2 mutant mice were able to remain on the inverted grid for average 19 seconds in contrast to their littermates that were holding on for average of 48 seconds (T test $p < 0.002$). In order to determine whether this inability persists in older

animals, the mice were re-tested at P28 and P35. At this stage there was no difference between groups, all subjects remained on the grid the entire testing time. The observed phenotype can be explained by a muscle weakness or reduced grip strength observed in the mutant mice early in development. To examine this possibility, grip strength measurements in another animal cohort were performed using “Digital Grip Strength Meter” (Columbus instruments International Corporation). In this test, a force in Newtons is recorded when a subject that holds on to the metallic bar is pulled away by its tail. Due to the possible sex related strength differences, males and females were considered separately. This analysis supported the inverted grid findings showing a grip strength reduction in mutant mice that persisted until four weeks of age and was no longer observed at P35 (Fig.4-1). This disparity can be explained by the significant force increase from P21 to P28 observed in both animal groups, which is probably sufficient to successfully perform the grid task. Both assays confirm that observed grip strength deficits in mutant mice result from developmental delay and are no longer detectable at P35. It can be speculated that mutant mice early in development display a hypotonia. Since high levels of IB2 are found in cerebellum the lack of thereof may result in cerebellar dysfunction. Cerebellum receives information from the muscle spindles through spinocerebellar tract and sends information through cerebrocortical tract to the motor cortex. Some disturbances in this signaling may result in cerebellar hypotonia. It may happen that motor cortex compensates for this insufficiency by increasing its activity, which could result in a disappearance of the hypotonia in mutants later in development. In humans it may happen through physical therapy, in mice perhaps during their normal activities they perform in a cage in order to compete for food and move around, which increases when they are weaned from their mother at

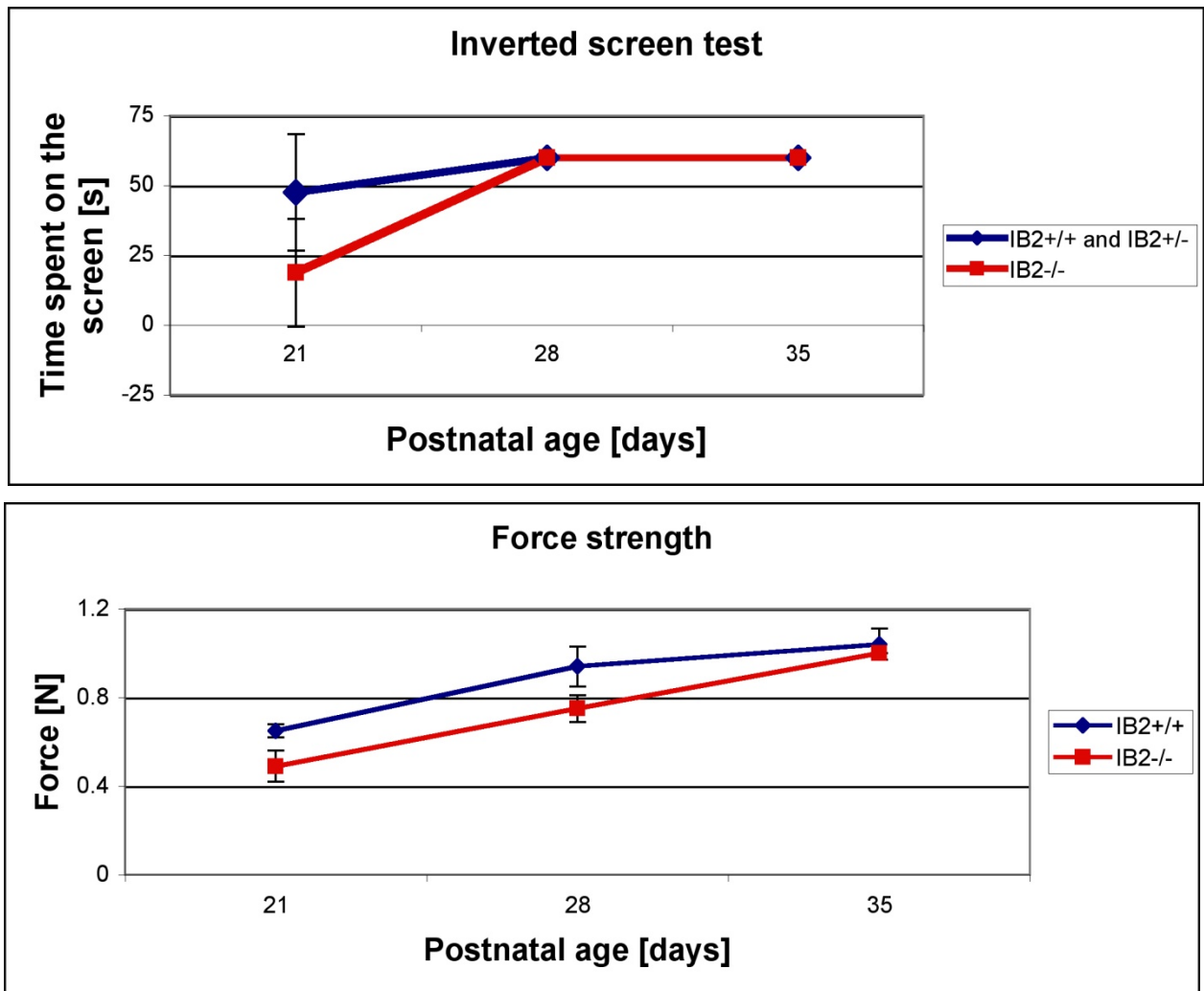


Fig.4-1

Developmental delay in grip strength. The ability of mice (on a mixed background 129Svev C57black6) to remain on the inverted grid was tested for 60 seconds. IB2 knockout mice fall off faster than wild types at three weeks of age, but at P28 they remain on a grid for entire 60 seconds (top figure). This is paralleled by the grip strength deficits observed at 21 days, which still persist at four weeks of age, but the significant force increase in that week may be enough to allow them perform well in the inverted screen task. Force strength differences are no longer observed at P35.

P21. This finding urged us to perform analysis of another cerebellum related phenotype. In addition, these results defined the age group for animals being used in subsequent analysis to be P35 or older.

Motor learning and fine motor skill deficits: Rotorod assays

To further explore possible cerebellum related deficits, we decided to subject the mice to the rotorod. This assay tests basal and learned performance in the complex motor skill of remaining balanced on an accelerating rotating horizontal rod. The skills necessary to master this task are a proper motor learning and fine motor movement coordination, both directly linked to cerebellar function.

Mutant mice and their littermates were familiarized with the apparatus for three times on a first day for a brief period of time. The testing began the next day and the mice were trained three times a day for 4 consecutive days on the rotorod where the speed was linearly increasing with time for a total of 360 seconds. The maximum rotation speed that mice could master was recorded and averaged from the three trials for a given day performance. Females and males were considered as separate groups in this task and a female example is presented. These mice were on a nearly pure 129Svev background backcrossed for seven generations (the same results were observed for the mixed background group, data not shown). The analysis was done first in a different testing area and then repeated in a home room for the reasons that will be discussed later in this chapter. Overall, IB2 knockout mice showed significant deficits in this task in comparison to their littermates (Fig.4-2). Their performance was much worse to begin with on a first day. Over the next four days wild mice significantly improved whereas mutant animals were not able to learn this task and their performance was

basically the same on the last and first day. Poor initial performance most likely corresponds to the deficits in fine motor skills and coordination. Furthermore, nearly completely absent progress in the mutant group tested in another room and a mild improvement observed in a home room clearly indicate their motor learning deficits. Overall, these results are a reflection of improper cerebellar functioning whether in its circuitry or on the signaling level.

Reduced conditional fear learning

Dramatic impairment in motor learning in IB2 knockout mice raised the possibility that another form of learning may also be affected. Since IB2 is highly expressed in amygdala, which is known to participate in an emotional learning and fear responses, we employed the use of a well described and commonly used elevated T-maze apparatus. This assay examines the fear and stress responses in rodents based on their innate fear of open spaces. The elevated apparatus is composed of one enclosed arm and two perpendicular open arms, where animals can be tested for conditioned fear (open arm avoidance so called inhibitory avoidance) and unconditioned (innate) fear (open arm escape-one way escape) (Echeverry et al., 2001; Jardim et al., 1999). In the inhibitory avoidance, a mouse is placed in the enclosed arm where it feels safer and once it positions itself facing the removable door that encloses this compartment, the door is removed and a mouse is allowed to explore open arms. It eventually learns to avoid it due to its innate fear of open spaces. In one way escape, on the other hand, the animal is placed at the end of an open arm and learns to escape from it based on the same principle. Both tests are performed using naïve mice and are conducted for 5 minutes during which an animal is allowed to freely explore the apparatus and while being

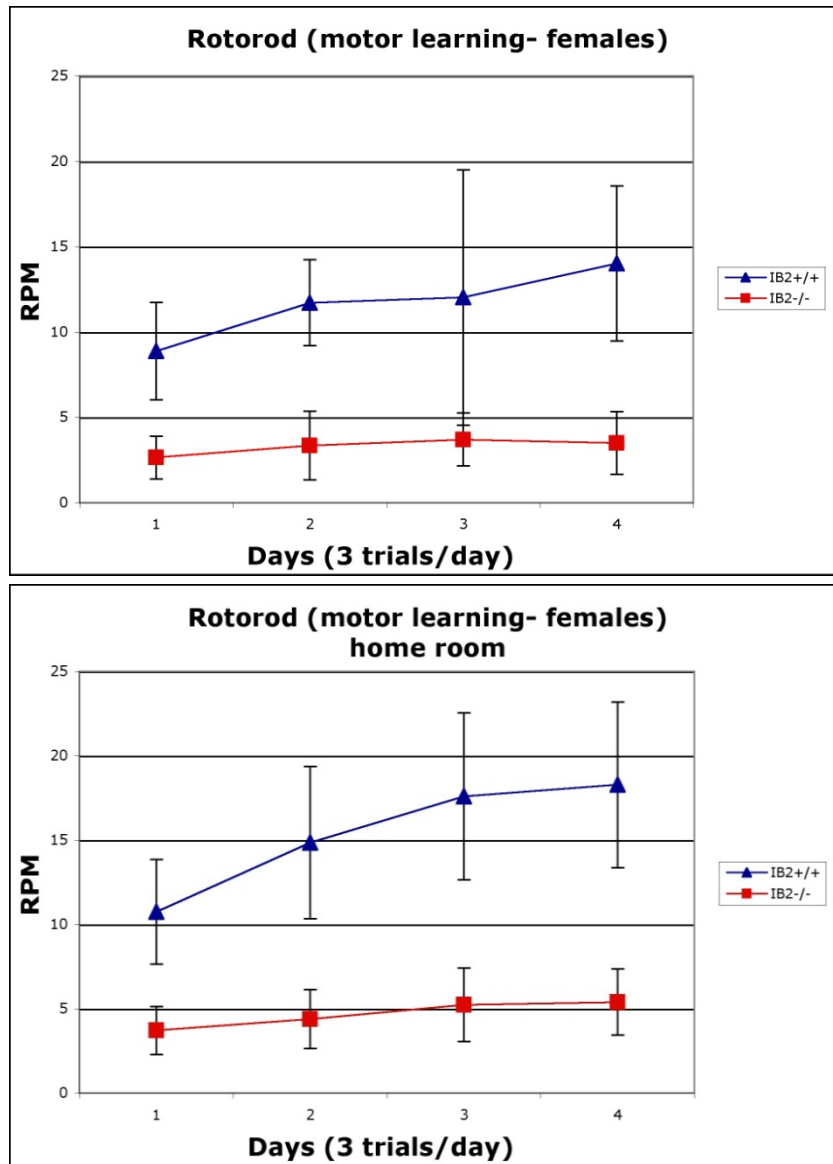


Fig.4-2

Rotorod. The mutant mice on a pure 129Svev background tested in a procedure room and in home room show impaired performance and motor learning in comparison to the wild type animals.

videotaped without the experiment administrator in the room. The time the mice spend in each arm is recorded and analyzed over three consecutive days.

Mutant mice showed impaired responses in both of these assays. However, their more complex behavior in the one way escape will be discussed in a further section of the behavioral chapter for clarity reasons.

In the inhibitory avoidance that examines conditioned fear responses, all wild type and heterozygote mice spend most time in the enclosed location and learn to fear and avoid open arms already on the first day of testing in contrast to the IB2 knockout animals, whose response appears to be rather random (Fig.4-3; top left panel). The Student's T test value for this day indicates high statistical difference between groups $p < 0.003$. They do not respond as a cohort in a similar manner, but rather wander around. Some spend more time in the open than others and are slower to learn. The number of exits into the open does not differ between mutants and their littermates (Fig.4-3; right top panel) and their locomotor activity is the same (data not shown). On the second day, however, they begin to show a trend as a group, spending more time in the enclosed location and finally on the third day they all avoid the open area similarly to their littermates. This delay in learning a negative response to the open arm strongly suggests a deficit in fear conditioning in IB2 knockout mice. Furthermore, it may also be a reflection of the difference in fear responses in this animal group. Alternatively or perhaps additionally, the lack of IB2 in the occipital lobe, where it is highly expressed, affects the visuospatial processing that may also contribute to this phenotype.

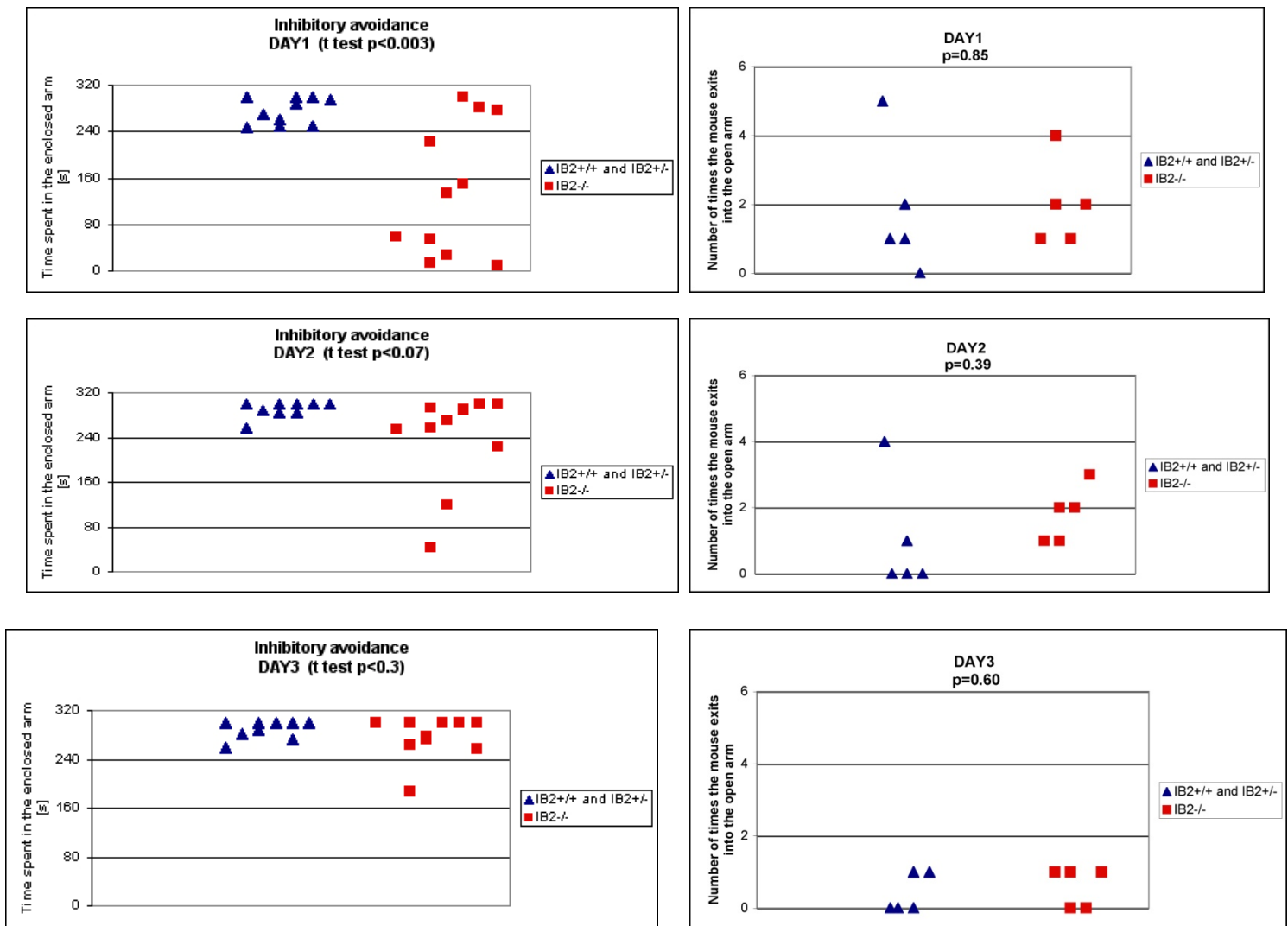


Fig.4-3

In the T-maze inhibitory avoidance test mutant mice on a mixed background show impaired learning abilities. When first placed in the enclosed location, they eventually learn to avoid an open region, but it takes them longer than wild type animals that learn this behavior on the first day.

Deficits in social interactions

The deficit in fear related conditional learning and possibly in innate fear in our mutant mice could result from defective functioning of amygdala. This part of the brain is also involved in other form of behavior such as social interactions. Lesions in amygdala in primates cause strong deficits in social contexts and are used as a model for human autism behaviors. Since some phenotypes in human 22q13 deletion syndrome are very similar to autism spectrum disorders and we suspect IB2 involvement in these diseases, we decided to examine IB2 mutant mice social interactions.

For this purpose, we performed social interaction test in a neutral environment. In this assay an animal pair (either mutants or wild types/heterozygotes) is placed in a neutral cage and allowed to interact for 10 minutes with the experiment administrator out of the room. A normal behavior in this context is for animals to explore one another by sniffing and/or touching with the tail. The amount of time the animals spend engaged in this behavior was recorded and analyzed. The female pairs and young male pairs were tested. The pairs of older males were omitted due to possible aggressive behavior. The data are presented as females only (Fig.4-4; left panels) or males and females data combined (Fig.4-4; right panels). IB2 knockout mice show significant impairment in social interactions under these circumstances. They spend on average about two minutes interacting as oppose to their littermates that engage in this behavior for almost twice as much time. This phenotype is typical of the entire cohort of pairs as can be seen on the bottom panels, which are just a different representation of the same data shown in top panels. It further confirms deficits that can be attributable to some defect in amygdala.

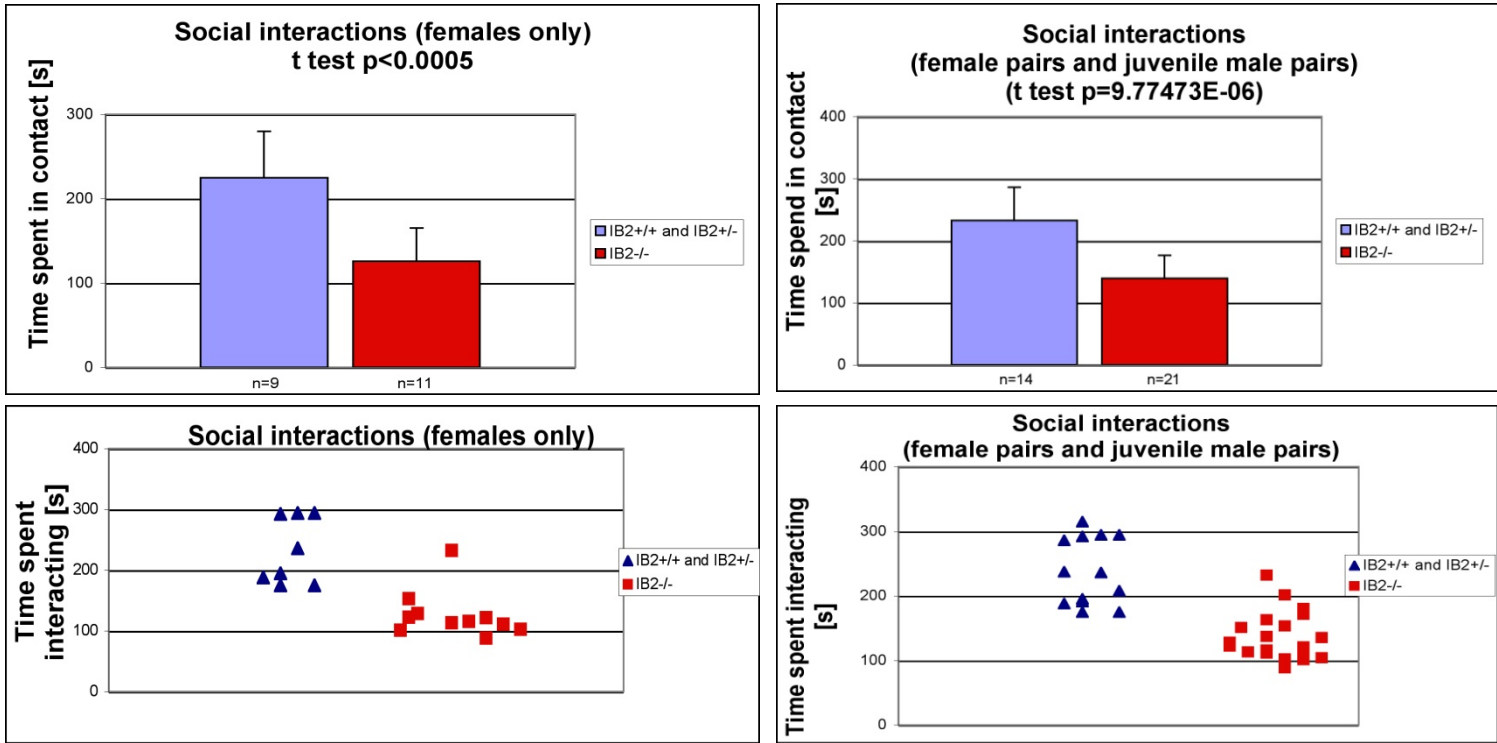


Fig.4-4

Mutant animals show reduction in social interactions. Females or juvenile males (P35) were placed in the neutral cages and allowed to interact for 10 minutes. The time spent interacting (sniffing, tactile contact by tail) was recorded. The left panels show different representation of the same data (females only) whereas the panels on the right show combined data (male pairs and female pairs).

Unresponsiveness to the environment in a subset of mutant subjects

As previously described, some of the conducted assays were guided by former results and in part by the phenotype found in 22q13 human genetic disorder in which an allele of *Ib2* is usually missing. However, because very little is known about IB2 function, a broad behavioral survey was also conducted. This analysis unexpectedly revealed another mutant behavioral phenotype: nonresponsiveness to environment. The assays presented in this section include novel object exploration, open-field locomotor activity, and dark-and-light paradigm.

The Novel Object Recognition test examines general exploratory behavior and the response to the new object. In this assay, a mouse is placed for 15 minutes in a square box (75x75cm) with an open top that contains two objects for two consecutive days. On the third day after 5 minutes of exploration, one of the old objects is exchanged for the new one and the mouse is allowed to explore for the next 15 minutes. The number of approaches to the new object and the number of approaches to the old object are recorded and analyzed. In the open field assay, a mouse is placed for 30 minutes in the clear guinea pig cage (19x16.5 inches) in the middle of the field and allowed to freely explore the area without experimenter in the room. This test is designed to measure locomotor activity, hyperactivity or exploration. Dark and light paradigm measures both spontaneous exploratory behavior and mouse natural aversion to brightly illuminated areas. As such, it allows for testing the exploration of the new environment, fear, and anxiety. A mouse is placed in the box with a partition, where half of the box is brightly lit and the other is a dark enclosed compartment. The mice being natural explorers would be expected to go in and out while spending more time in the dark area where they feel less anxious (Hascoet et al., 2001).

When these assays were performed, as well as the one way escape from the elevated T-maze, the mutant mice group showed significant statistical difference from their littermates (Fig.4-5). However, closer examination of the data interestingly indicated that this difference is attributable to a certain percentage of mutant animals that display atypical behavior. They appear completely unresponsive to the environment. They simply stay exactly where they were put by the experimental investigator (myself) and remain there for the entire length of the performed test. Their behavior cannot be categorized as freezing since they are moving their front paws or turn around, but staying in the same area without four-legged walking, as if they were lost. In each of the figures corresponding to the different assay, these animals are outlined with the red square. Interestingly, a common feature of these tests is an open space in new surroundings.

In the T-maze one way escape that measures the innate fear response, several subjects beginning on the first day remain on the open arm region where they were first placed and never learn to escape from it into the enclosed area since they have never learned about the existence of such location. The rest of analyzed mutant animals behave in a similar manner to their littermates displaying gradual learning over three days and spending nearly entire time in the enclosed arm on the last day of testing (Fig.4-5a). Upon removal of the unresponsive subjects, the Student's t test analysis shows no differences between groups (data not shown).

Similarly, in the novel object recognition test (Fig.4-5b), a group of knockouts shows complete lack of exploration of either old or new object. None of the wild type subjects behaved in this fashion during this assay as exploration is an inborn rodent characteristic. The rest of mutants, once again, shows similar response to the wild type group.

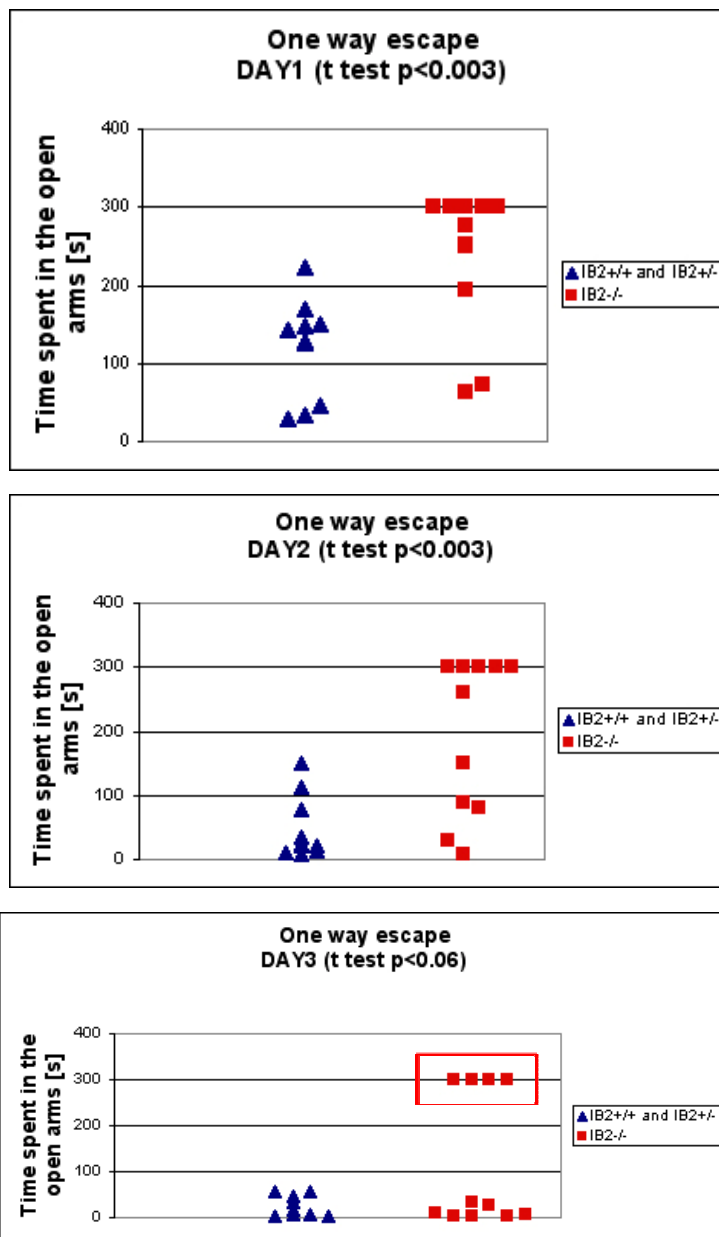


Fig.4-5a

Nonresponsive phenotype observed in the subset of mutant mice in one way escape in T-maze apparatus.

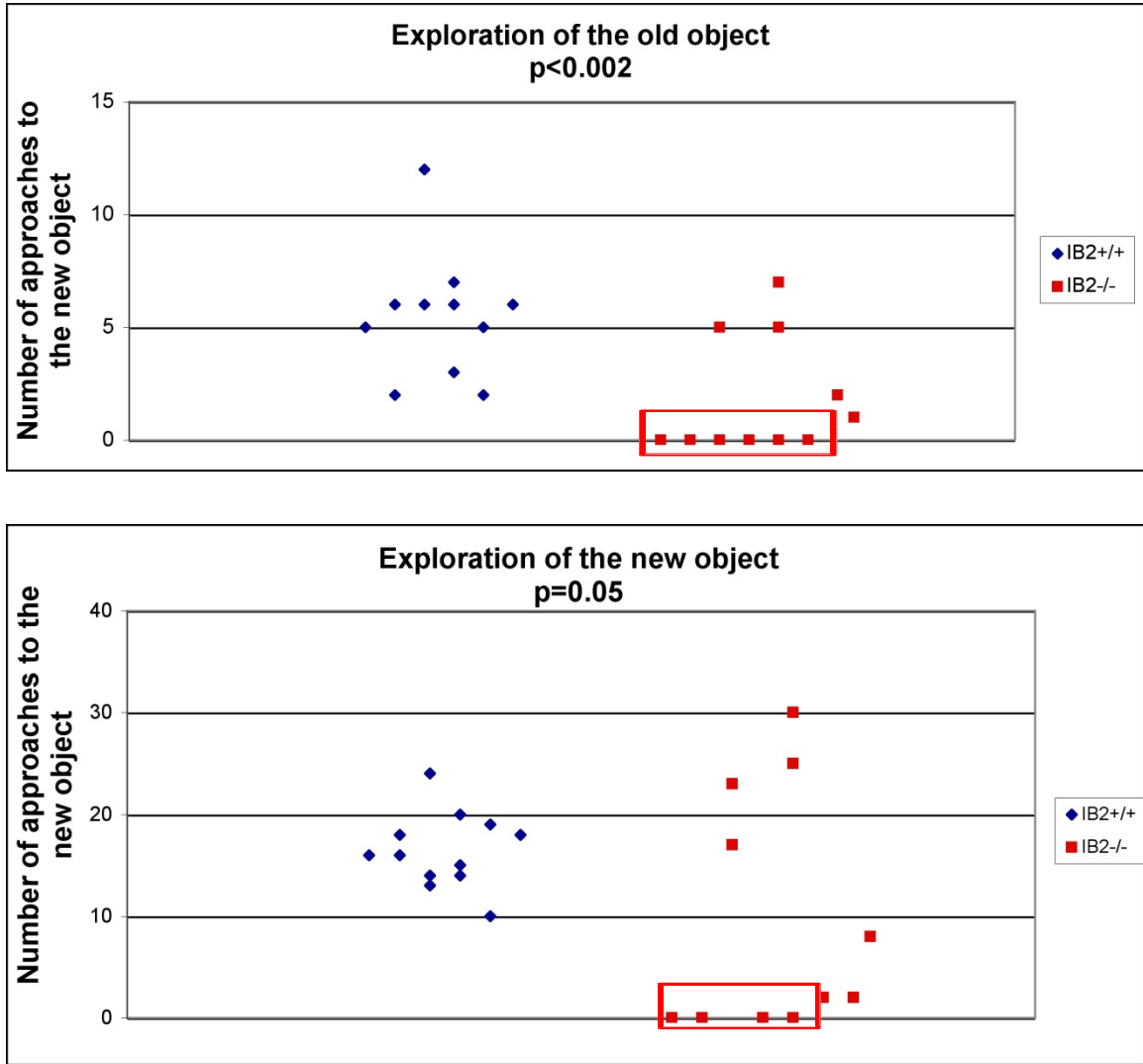


Fig.4-5b

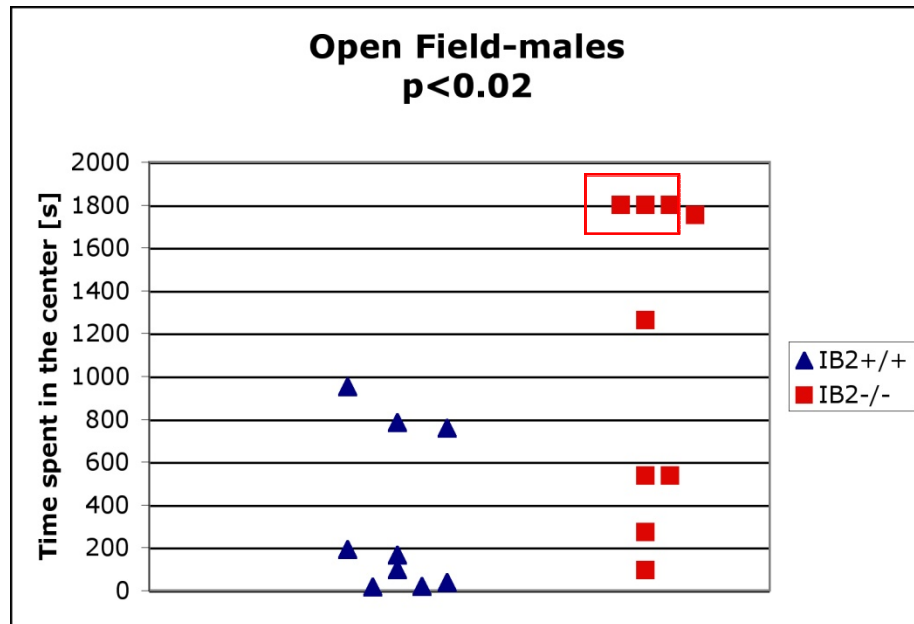
Nonresponsive phenotype in the subset of mutant mice in Novel Object Recognition test.

In the open field assay (Fig.4-5c), a subset of IB2 knockout mice simply stayed at the center location where they were first placed and did not move for the entire 30 minutes assay even though the area near the walls would be a safer choice. Once again, there was no wild type animal that would display this kind of behavior.

Finally, in the dark and light paradigm (Fig.4-5d) where the mice are also allowed to explore their surroundings and encouraged to enter the dark area by the mild stressor in a form of the bright light, several mutant subjects remained for the entire assay time in the light. This behavior argues against increased anxiety, since they would rather escape this area unless their anxiety level is so high that it makes them unable to move. The rest of the group also acted as their wild type counterparts.

The differences in mutant group responses in these assays could not be attributed to factors such as sex, age or testing during the light cycle. Males were used in open field and dark and light paradigm, females in novel object exploration and both in T-maze analysis. All animals were in the same age group range P35-P49 and each animal in a given assay was tested during the similar time of a light cycle (in the afternoon) and in the same procedure room. All were handled by the same investigator (myself). The nonresponsiveness of mutant animals in the above assays also cannot be attributed to an inherent impairment of locomotive capability. In a similar open-field assay performed in the home room as opposed to a procedure area, all mutant animals were active (data not shown). Furthermore, when these same animals were re-tested in a separate procedure area over several days, most mutant animals became non-responsive (Yam, Giza and Goldfarb, data not shown). Therefore, nonresponsiveness was not apparent when mutant animals were in a familiar environment, but was a trait developed when faced with (stressed?) novel environment.

c)



d)

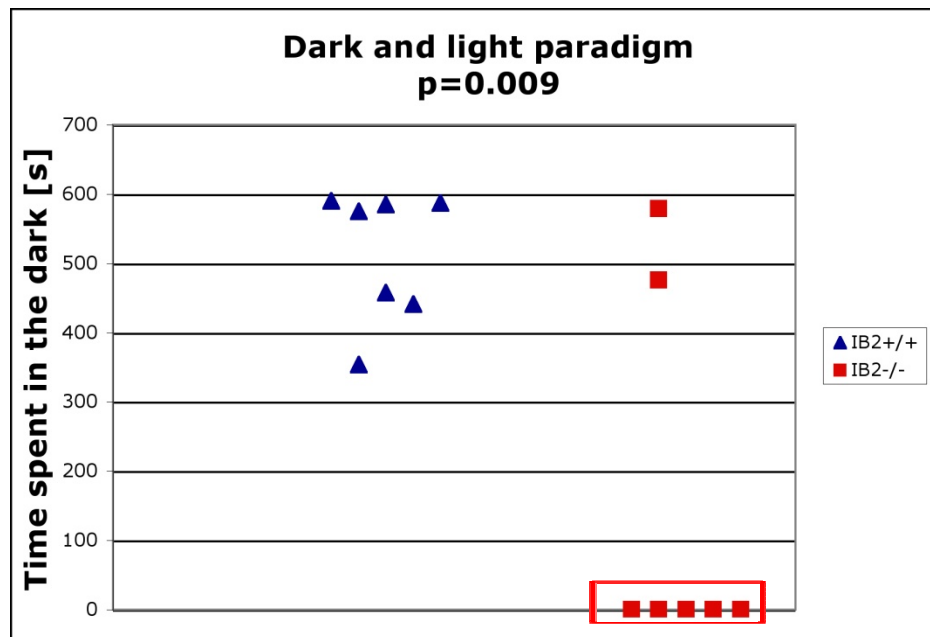


Fig.4-5c,d

Nonresponsive phenotype in the subset of mutant mice in open field and dark and light paradigm assays.

Discussion

IB2 mutant mice showed deficits in multiple neurological processes indicating the need for this protein for a proper functioning of the nervous system. Interestingly, many of them resemble human Phelan-McDermid Syndrome. The children with this disease, among others, often display hypotonia, motor learning and motor skills impairment, difficulty to communicate and interact socially early in development, unresponsiveness to the environment and deficits in amygdala shown by positron emission tomography. IB2 knockout mice display inability to remain on the inverted grid and grip strength deficits that may result from hypotonia manifested as a developmental delay, possibly due to other molecules and/or other brain areas compensatory effects later on. The motor learning and coordination are significantly impaired as shown in their poor rotorod performance. It is known that cerebellum dependent motor learning requires proper long term depression (LTD). Interestingly, IB2 binding partner, p38MAPK has been implicated in this process. It is possible that the lack of IB2 might affect LTD either through p38 or other means. LTD in IB2 mutant mice is currently being analyzed by our collaborators. Juvenile mutant mice also display a marked reduction in social interactions, a finding that could point to defects in amygdala. Alternatively, it could be explained by olfactory deficits, which is currently under investigation in our laboratory. As a possible reflection of additional amygdala malfunctioning, *Ib2* knockout mice show abnormal response to fear conditioning or fear in inhibitory avoidance in T-maze apparatus. The most peculiar phenotype observed in a subset of mutant mice is unresponsiveness to environment, which could stem from deficits in sensory information processing and/or individual responses to stress. The vision in *Ib2* mutant mice appears to be intact as they are able to successfully navigate to a visual platform

during Morris Water Maze analysis (data not shown). It can be speculated that the unresponsiveness to the environment observed only in some mutants is a reflection of an incomplete penetrance of *Ib2* gene deletion. The uniform performance of mutants as a group in other assays may be a reflection of *Ib2* pleiotropy and different necessity levels for this molecule in various processes and/or in distinct regions of the brain. IB2 in a wild type is widely but not uniformly expressed throughout the brain (Negri et al., 2000). Alternatively, this finding could be explained by strong emotional stimuli and responses evoked in these assays and the differences among animals in coping with stress. If the animal's emotional reaction is compromised to begin with as we suspect is the case in IB2 knockout mice since they display deficits in amygdala related tasks, its response to the stressful stimuli such as novelty and open space may also depend on additional personal traits. Some may have naturally higher resistance to stress while others may not, which could contribute to different responses to the same situation. Thirdly, there is a possibility that the lack of IB2 in some animals depending on their personal experiences have been randomly compensated by other molecules or mechanisms. For instance, a visuospatial deficits in occipital lobe and inability to orient in space due to cerebellar deficits may be compensated for visual and motor cortex area increased intrinsic excitability, which may depend on animals' personal experiences such a singly housed versus crowded cage, very few or multiple sibilings and competition for food and space during development. It may be supported by the finding that in some of our assays, performed in a home room, mutants behave as their wild type counterparts (Giza and Yam, unpublished data). It is possible that additional stressor in a form of a different testing area e.g. sensory, visual and odor stimuli are enough to push some of the mutants over the edge to display certain behavior that under normal conditions would go unnoticed. As the function of IB2 becomes clearer, it may be easier to explain mutant mice performance under

certain circumstances. Due to these last two characteristics, the 22q13 deletion syndrome is often misdiagnosed and mistaken with other most commonly known autism spectrum disorders. It is also one of the reasons why this syndrome is still poorly described and so few subjects were being studied. Nevertheless, nearly all described patients display above features. Therefore, the lack of *Ib2* in human deletions may contribute to some of the features or have synergistic effects with other missing genes in this disease. These findings together with IB2 exclusive nervous system expression are suggestive of its neurological function and argue that *Ib2* knockout is a mouse model for human Phelan- McDermid syndrome.

CHAPTER 5

MOLECULAR AND CELLULAR ANALYSIS OF IB2 MOLECULE

Introduction

In spite of IB2 sequence similarity to IB1 (JIP1) and its ability to interact with JNK kinase *in vitro*, current reports regarding its cascade scaffolding abilities, protein-protein interactions and localization remain controversial (Yasuda et al., 1999; Negri et al., 2000). Its expression along with other components of JNK MAPK cascade potentiated JNK activation in a similar manner to JIP1 and overexpression inhibited JNK activation suggesting its involvement in this signaling pathway (Yasuda et al., 1999). However, IB2 was unable to compensate for the lack of IB1 in JIP1 knockout mice and the JNK signaling in these animals was impaired (Whitmarsh et al., 2001). Other laboratories showed that IB2 binds to JNK is very weak and it is in fact forming stronger complexes with another MAPKs, p38 α and p38 δ , and can interact with their upstream activators MKK3 and MLK3 (Robidoux, et al., 2002; Schoorlemmer and Goldfarb, 2001). In these studies IB2 was shown to potentiate p38 α and δ activation upon interaction with its distinct binding partners TIAM1 and FHF's respectively, both of which do not associate with JIP1. TIAM1 is a guanine exchange factor specific for Rac1, which is upstream from MLK3. Early in development it can be found at the growth cone, but in mature neurons, it localizes to dendrites (Tolias et al., 2005). FHF's are involved in regulating intrinsic excitability of neuronal cells and can be found interacting with sodium channels at the axon initial segment. Their interaction with IB2 and sodium channels is mutually exclusive. In presence of IB2, FHF's potentiate activation of p38 δ in a dose dependent manner. Endogenous complexes of IB2 and TIAM1 or FHF's are found in the

brain protein lysates. In addition to aforementioned interactions, IB2 contains additional array of binding partners such as amyloid β precursor protein and apolipoprotein E receptor. Noteworthy is also its interaction with the motor protein kinesin which suggests its delivery to the tips of dendrites and/or axons in a manner similar to JIP1 (Verhey et al., 2001).

The vast array of the binding partners and potential involvement as a scaffold for distinct signaling cascades make it very difficult to approach IB2 analysis. We hypothesized that as a binding partner of TIAM1 and JIP1 which are found localized at the dendritic tips and as a kinesin cargo IB2 also has a potential to reside and be delivered to the postsynaptic regions. There, it could participate in a signal transduction leading to activation of p38 MAPK, which is known to be strongly enriched at this site. Interestingly, both p38 and TIAM1 were implicated in NMDA receptor dependent synaptic plasticity. TIAM1 is phosphorylated in response to NMDA receptor activation, a process which results in spine outgrowth and formation. p38, on the other hand, is involved in the NMDA receptor dependent learning and memory processes such as LTD and LTP early in development under certain circumstances (Kennedy et al., 2007). Therefore, we have turned to investigate the presence of IB2 at the synapse and examine p38 signaling pathway and TIAM1 induction following the NMDA receptor activation as possible key events in IB2 functioning.

Results

This chapter will demonstrate the evidence that IB2 is a resident of a postsynaptic density (PSD) as shown by brain fractionation, co-immunoprecipitation with PSD components and by immunostaining. No differences in basal levels of the common PSD residents were found in the IB2 knockout mice. p38 MAPK basal and active levels also did not differ. In addition,

no deficits have been found in a signaling pathways previously reported to result in p38 and TIAM1 activation upon NMDA receptor stimulation, showing no involvement of IB2 in the signaling from NMDAR to p38.

Generation of a mouse monoclonal antibody against IB2

In conjunction with NeuroMab Facility (Antibodies Incorporated) we were able to generate mouse monoclonal antibody against IB2 molecule that is specific for IB2 and does not interact with JIP1. We have provided the company with the immunogen His6-mIB2 containing residues 226-421 that bear no sequence homology to JIP1 as well as plasmids expressing full length flag tagged IB2 and JIP1 and rabbit anti-IB2 peptide antibody. Several clones of this antibody were tested using brain protein extracts from our wild type and IB2 knockout mice and the clone that gave the strongest signal was chosen for our subsequent analysis (data not shown). The monoclonal antibody recognizes IB2 molecule which runs in the polyacrylamide gel at the 150 kDa, which is in agreement with the previously used peptide antibody. The normal size of IB2 is about 75kDa protein, but various posttranslational modifications could account for its noticeable gel shift.

IB2 presence in the brain

It has been shown previously by Northern Blot analysis that IB2 is expressed widely in the brain (Yasuda et al., 1999; Negri et al., 2000). In order to confirm that the IB2 protein is indeed present in multiple murine brain locations, protein extracts were prepared from various brain regions of IB2^{+/+} mice and Western Blot analysis was performed using

extracts from knockout mice brains as a negative control. Indeed, the presence of IB2 was found in regions including olfactory bulb, cerebral cortex, midbrain , brain stem and cerebellum (Fig.5-1).

IB2 enrichment at postsynaptic density

IB2 interacts with TIAM1, a Rac1 guanine nucleotide exchange factor present at growth cones and at the dendritic tips. TIAM1 is involved in dendritic growth and spinogenesis, most likely through its effects on Rac1 activation and actin remodeling (Tolias et al., 2005). IB2 also binds to p38 MAPK, which has been found in high levels at the postsynaptic density and which participates in LTD related to the processes of learning and memory (Li et al., 2006). In addition, as other JIPs, IB2 possesses TPR motifs to interact with motor protein kinesin. Therefore, we hypothesized that as a result of these interactions IB2 may also localize to PSD regions. We examined this possibility through fractionation experiments. For this purpose, hippocampi and cortices were dissected out from wild type and mutant mice and subjected to homogenization and subsequent fractionation steps. The fraction 1 (crude lysate) contained the starting homogenate and was subjected to the centrifugation in a sucrose gradient (1.25M:1M:0.32M) in order to collect the synaptosomes (SYN: fraction 2) that contain the cell membrane and synaptic proteins. Synaptosomes were then solubilized with nonionic detergent, from which the insoluble high-speed pellet constituted the postsynaptic density (PSD: fraction 4). Western Blot analysis of the fractions was performed by loading the same amount of proteins and blotting with antibodies against

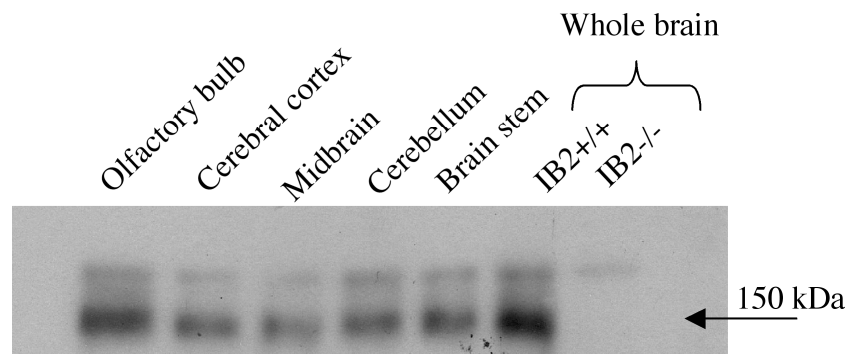


Fig.5-1

Protein extracts were prepared from different brain regions of a wild type mouse. IB2 protein can be found throughout the brain. IB2^{-/-} lysates were used as a negative control.

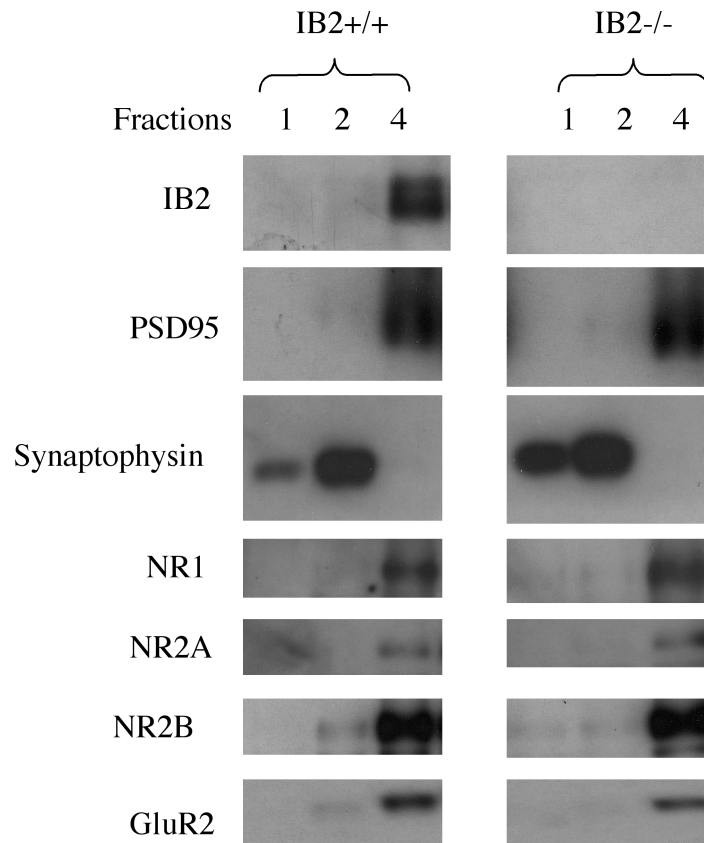


Fig.5-2

Brain fractionation shows co-enrichment of IB2 with postsynaptic density elements: postsynaptic density protein 95 (PSD95), N-methyl-D-aspartate receptor (NMDAR) subunits NR1, NR2A, NR2B and glutamate receptor subunit GluR2. Synaptophysin was used as a presynaptic marker and therefore, it is absent from the PSD fraction. The levels and distribution of PSD components appear to be unaffected by the lack of IB2.

classical markers of pre- and postsynaptic density (Fig.5-2). As expected, the presynaptic marker, synaptophysin is enriched in synaptosome fraction 2 in comparison to homogenate fraction 1 and is missing from postsynaptic density fraction 4. Conversely, very high levels of the classical marker of PSD, a scaffold protein called PSD95 is can be observed in the PSD fraction together with the subunits of the NMDA receptors (NR1, NR2A, NR2B) and AMPA receptors (GluR2), that are known to be localized at the PSD membrane. As we suspected, IB2 is strongly enriched at the postsynaptic density fraction. In these experiments, the fractions from IB2 knockout mice were used as controls. The localization and amount of pre- and postsynaptic components in IB2^{-/-} do not seem to be affected, arguing against substantial IB2 involvement in their distribution and/or expression.

IB2 associates with postsynaptic density elements

Since IB2 turned out to be enriched at PSD we wanted to find out whether in fact it interacts with postsynaptic density elements. To test this possibility, IB2 was immunoprecipitated from the wild type and for control purpose knockout brain lysates and subjected to Western Blot analysis using antibodies against previously described PSD residents (Fig.5-3). TIAM1 was used as a positive control as it has been previously shown to interact with IB2 (Buchsbaum et al., 2002). Indeed IB2 immunoprecipitation pulled down TIAM1 (bottom panel) as well as NMDA receptor subunit NR2B along with AMPA receptor subunit GluR2 and scaffolding molecule PSD95 (Fig.5-3). At the postsynaptic density, AMPA receptors interact with GRIP protein whereas NMDA receptors bind to PSD95. Both GRIP and PSD95 interact with SHANK, which is thought to organize AMPA and NMDAR

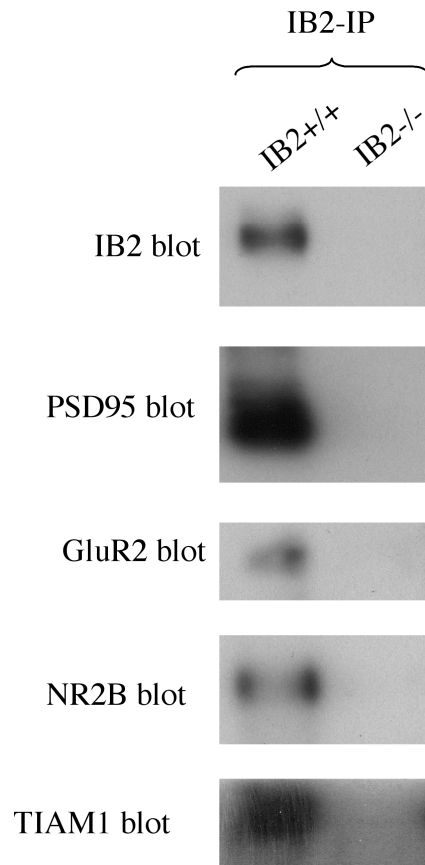


Fig.5-3

IB2 co-immunoprecipitates with postsynaptic density elements such as PSD95, GluR2 and TIAM1. TIAM1 also serves a purpose of a positive control since it has been previously described to interact with IB2.

at the intracellular level, since it lies further from the cell membrane (Sheng and Kim, 2000). The fact that these molecules are a part of strongly associated network of binding partners may result in IB2 pulling down all of them under these particular conditions.

IB2 is present in dendritic spines

In order to confirm that IB2 is in fact present at PSD we performed the immunofluorescence analysis in three week old rat hippocampal neuron cultures. The outline of the neuronal cell was demarcated with the anti-tubulin FITC conjugated antibody (green). Tubulin is absent from the dendritic spines, which are filled with actin that was visualized with phalloidin-rodamine (red). IB2 was detected using mouse monoclonal anti-IB2 antibody and visualized with the anti-mouse Cy5 secondary reagent (Fig.5-4). IB2 is indeed present in spines where other PSD components are known to localize. It can also be seen in structures along the dendrites that might be vesicles suggesting its active transport within the dendritic compartment. We have also detected IB2 presence at the growth cones of immature neurons in cultures (data not shown). Both findings are consistent with IB2 being a cargo for kinesin that delivers towards the plus end of microtubules (Verhey et al., 2001). We have also repeated the immunostaining using secondary antibody coupled to Alexa- 488 and demarcating the spines with phalloidin- rodamine that binds to actin in order to make sure that the above observation of IB2 in spines was not due to the artefactual spillover of the rodamine signal into the Cy5 detection window. Here, with IB2 (green) and actin (red), IB2 can be clearly seen within a spine (Fig.5-5). It appears to localize to the spine head where other PSD constituents are present and be absent from the constricted neck region.

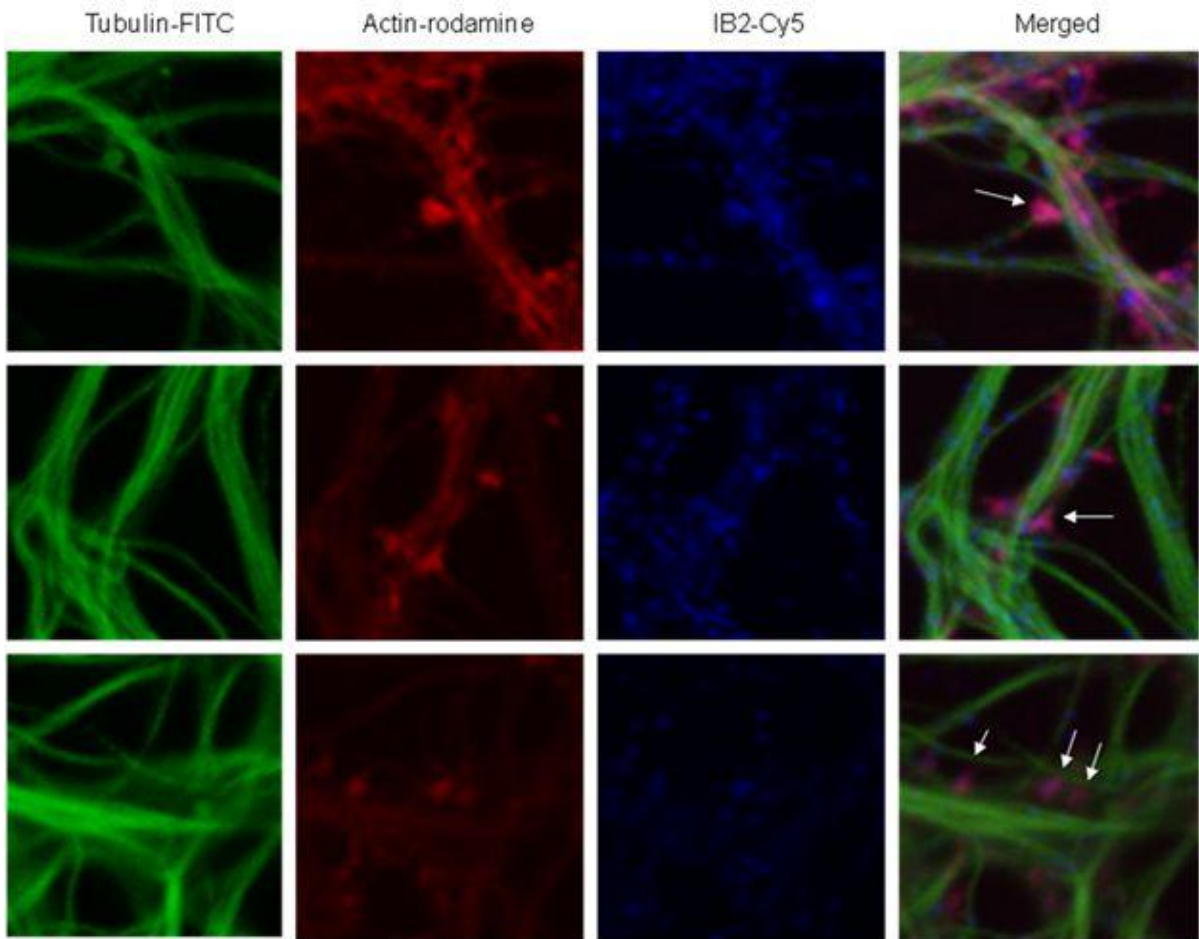


Fig. 5-4

Rat hippocampal neurons were fixed at DIV21 by 4%PFA at room temperature. Morphology of the neuronal processes is shown with tubulin (green) and the dendritic spines are shown with actin (red). IB2 is visualized with mouse anti-IB2 antibody using anti mouse Cy5 as a secondary reagent.

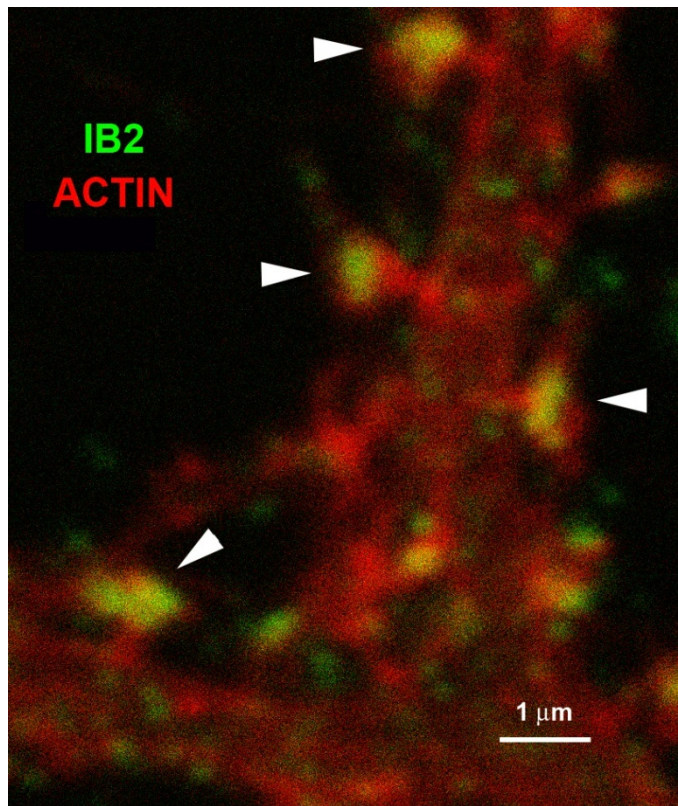


Fig.5-5
IB2 (green) can be found in spine heads (indicated by arrowheads) where it colocalizes with actin (red).

IB2 does not affect the basal levels of PSD components

The presence of IB2 at PSD may have multiple functions. One of the possibilities is that as a cargo for kinesin, it is needed to deliver its binding partners to the proper location. Delivery of the NMDA receptor subunits has been shown to depend on the molecule called Kif17 that also binds to kinesin. IB2 could serve as an alternative transport of these molecules and/or deliver them in response to certain pathway activation. Alternatively, as a putative scaffold, it could affect signal transduction and possibly the gene expression of NMDA or AMPA subunits and/or other PSD residents. However, the analysis of the basal levels of NMDA and AMPA receptors, PSD95 and TIAM1 in the brain extracts of IB2 knockout mice showed no difference in comparison to the wild type (Fig.5-6). Additionally, because the mutant mice showed strong deficits in a motor learning and performance pointing to the possible cerebellar learning defect, these levels were also examined in cerebellar extracts, including NR2C subunit which is specifically expressed in this brain region, but no deficits were observed (Fig.5-7). Furthermore, electron microscopy analysis performed by a collaborator Victor Friedrich (Mount Sinai School of Medicine) has shown no differences in synapse size and morphology in the cerebellar granule or molecular layers. However, electrophysiology recordings performed by other collaborators, Francesca Prestori and Egidio d'Angelo (University of Pavia), indicate elevated synaptic NMDA currents in cerebellar granule neurons from mutant mice. These changes could reflect altered distribution of NMDARs or altered unitary NMDAR conductance, perhaps through receptor modulation for example by phosphorylation.

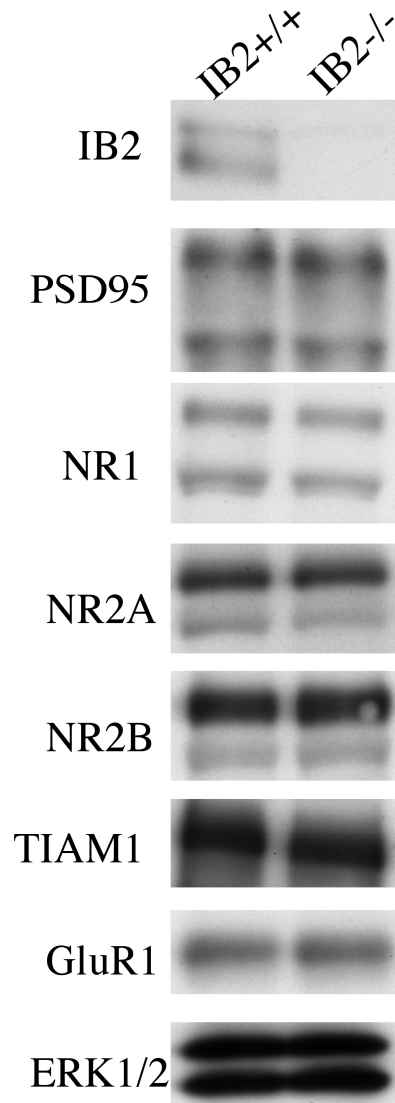


Fig.5-6

The basal levels of postsynaptic density constituents are unaffected in IB2 knockout mice as shown by Western blotting using whole brain extracts. ERK was used as a loading control.

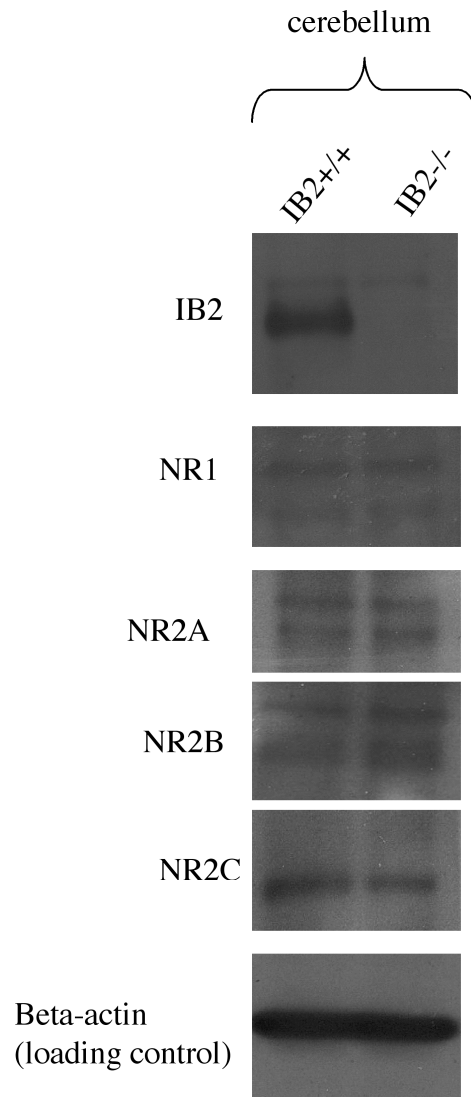


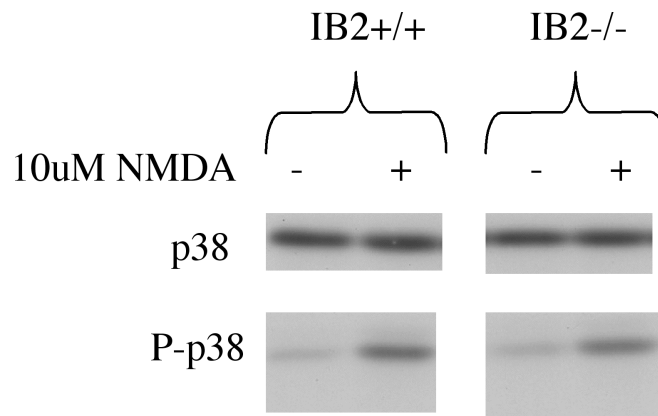
Fig.5-7

The levels of NMDAR subunits in cerebellum are unaffected in IB2 knockout mice brain.

IB2 is not essential for NMDA signaling to p38 and TIAM1

IB2 knockout mice behavioral deficits clearly implicate this protein in neurological function. The fact that IB2 localizes to PSD along with its binding partners TIAM1 and p38 MAPK, which were shown to be activated in response to NMDA receptor induction, suggested that IB2 may participate as a scaffold in this signaling. In order to test this hypothesis, cortical cell cultures were prepared using separately processed E18 embryos resulting from IB2^{+/-} matings. At DIV14 wild type and knockout cell cultures were treated with 10 μ M NMDA for 5 minutes in presence of glycine (necessary cofactor for NMDAR activation). The cells were then lysed, harvested and subjected to Western Blot analysis. As expected, p38 was phosphorylated in wild type cell culture in response to NMDA (Fig. 5-8a) and the same levels of phospho-p38 were observed in the mutant culture. The basal levels of p38 MAPK in these cultures did not differ. This experiment showed that IB2 does not participate in the signaling from NMDAR to p38 at least under these experimental conditions. We also looked at its basal phosphorylation levels in mice 2 weeks and 2 months of age, but still found no differences there (Fig.5-8b). Following these results, we turned to another finding in literature regarding another IB2 binding partner, TIAM1. TIAM1 was shown to interact with NMDAR and become phosphorylated upon calcium influx following the NMDAR stimulation. TIAM1 is a guanine exchange factor for Rac1. Activated Rac1 can then stimulate another IB2 partner, MLK3. In this case IB2 could serve as an adaptor bringing the TIAM1 to a proper location. Even though the levels of TIAM1 at PSD in the knockout do not differ from the wild type, it may be mislocalized and thus not phosphorylated in response to NMDAR activation. To examine this hypothesis, we stimulated TIAM1 as previously shown (Tolias et al., 2005) by adding 50 μ M glutamate to

a)



b)

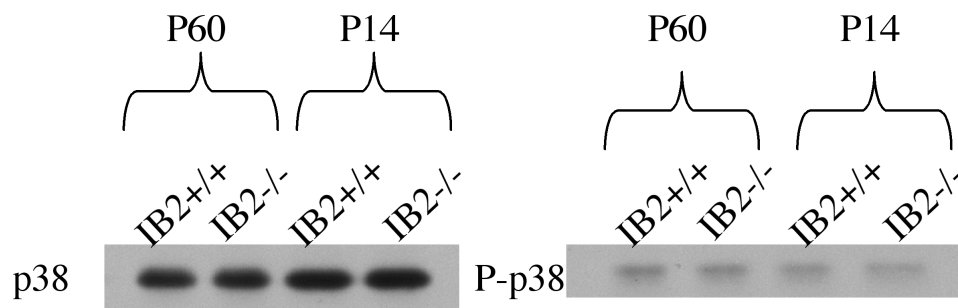


Fig.5-8

a)The levels of basal and activated p38 MAPK kinase in wild type and mutant cultures following NMDAR induction do not differ. b) The basal levels of p38 and phospho- p38 in the brain at different developmental stages: adult (P60) and pup (P14) are also the same.

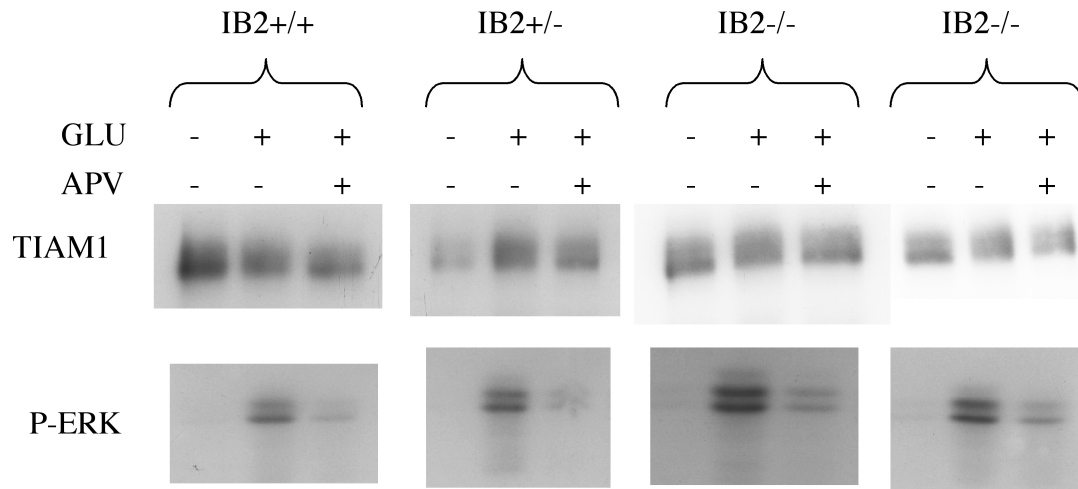


Fig.5-9

TIAM1 induction in cortical cultures prepared from wild type, heterozygote and mutant embryos. Cultures were stimulated with 50 μ M glutamate in presence of CNQX, TTX and nimodipine. The activation of ERK was examined to show that the stimulation experiment worked as it is known that ERK is activated in this pathway. APV, a selective blocker of TIAM1 activation reduced ERK activation and prevented TIAM1 activation. The stimulation of mutant cultures showed no difference in comparison to the wild type.

cultures to activate NMDARs. In order to ensure that this activation is due to NMDA receptor, other channels were blocked with appropriate inhibitors: TTX, CNQX and nimodipine. After 5 minutes, the cells were lysed and proteins were analysed by Western Blotting (Fig.5-9). The wild type, heterozygote and mutant cultures all showed induction of TIAM1 to a similar extent, which can be seen as a gel shift of phosphorylated TIAM1. In unstimulated control wells, the lower, unphosphorylated band is a predominant one similarly to the wells corresponding to APV pretreatment. APV is a selective blocker of NMDA receptor. Its pretreatment prevented TIAM1 activation in all tested cultures. If, as we hypothesized, TIAM1 in knockout cells would be mislocalized, it could still be phosphorylated by this treatment, but pretreatment with APV could not prevent this activation as it would not be due to NMDAR association. Taken together, these results show that NMDAR activation and signal transduction through MLK3-MAPKKK to TIAM1 do not require IB2. Suspecting that IB2 might be involved particularly in p38 δ signaling we have also analyzed TAU and eEF2 kinase- two known substrates for this p38. The phosphorylation status of these proteins at various developmental ages was also not altered in *Ib2* knockout mice (data not shown).

IB2 might be involved in neuronal branching

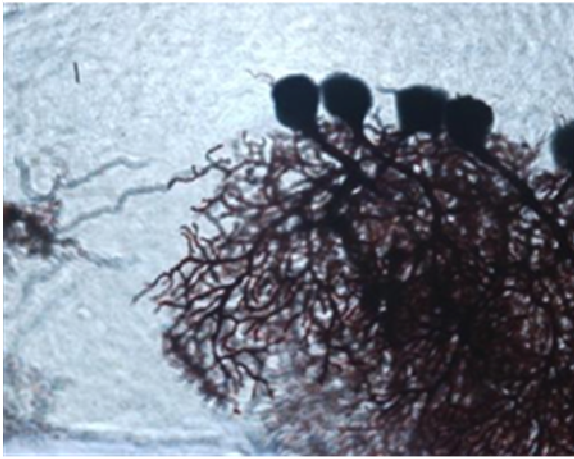
We showed that IB2 does not affect the expression levels of the PSD components or signaling cascades from NMDAR to TIAM1 and p38 MAPK. However, it may still be involved in signaling downstream from TIAM1, which has been implicated in dendritic branching and spinogenesis. Therefore, we wanted to know whether overall neuronal cell morphology is affected in *Ib2* knockout mice. The method that is often used to give a first

general estimate of cell morphology is a Golgi stain. We decided to use it in order to look at the dendritic tree in a Purkinje cell since it is the most arborized cell in the nervous system and the obvious differences could be easily spotted there. In addition, our behavioral analysis pointed to some deficits in cerebellar functioning. For this purpose, the brains of three week old mutant and wild type mice were fixed by transcardial perfusion. The cerebella were sliced in vibratome in potassium dichromate solution and the slices were incubated in the potassium dichromate overnight. Following this treatment, the slices were then developed in silver nitrate and fixed with xylene on the slides. Unfortunately, we were unable to stain single neurons and often observed the Golgi staining “hot spots” of multiple Purkinje cells which obstructed our overall analysis. An interesting feature that emerged was that the mutant dendritic tree appears to be shorter than that of the wild type animal and the dendrites seem to occupy less space, which can be seen here in a group of five neighboring Purkinje neurons (Fig.5-10). However, these data were not readily quantifiable. More recent fluorescent dye injection experiments in our lab demonstrated that dendritic arbors of mutant Purkinje cells are in fact shorter in addition to ~40% deficits in the dendritic volume (Urbanski, unpublished data).

Discussion

Using newly raised monoclonal antibody we were able to confirm that IB2 is present in distinct mouse brain regions, consistent with earlier RT-PCR (Negri et al., 2000) and Northern Blotting analysis (Schoorlemmer and Goldfarb, unpublished data). Interestingly, we found that IB2 is enriched at the postsynaptic density and is specifically present in spines. These structures are known to participate in synaptic plasticity related to processes such as learning and memory. For instance, their number increases during LTP and decreases during LTD. IB2 interacts with PSD elements such as AMPA and NMDA receptors that are known to participate in these events. Due to the nature of the PSD, however, any constituent can be found in a complex with IB2 as a result of immunoprecipitation. The examination of the direct association would require coexpression of the single components along with IB2 in the non-neuronal cells and analysis of their complexes there. We found no change in the basal levels of these components in the PSD fractions from IB2 knockout brains, although we cannot rule out subtle changes in component abundance or organization within the PSD scaffold. Additionally, NMDA induction and resulting p38 and TIAM1 activation was not affected in IB2 knockout neurons. It is still possible that IB2 participates in other signaling pathway from NMDAR. However, due to the multiplicity of binding partners along with very little knowledge and confusing reports regarding IB2 molecule, we have limited our analysis to the strongest leads in literature which were TIAM1 and p38. In addition, IB2 could have a redundant function in bringing its binding partners to the PSD, which is taken over by other molecules in its absence or it is only involved in these processes in a specific single pathway.

IB2+/+



IB2-/-

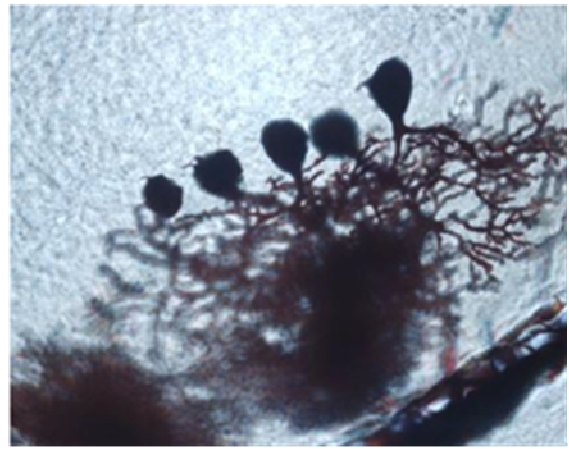


Fig.5-10

Golgi staining of Purkinje neurons in slices of three week old wild type and knockout mice cerebella.

CHAPTER 6

DISCUSSION

IB2 has been previously described as a putative kinase scaffold protein. Scaffold protein levels have to be correctly adjusted by the cell in order to properly function. This characteristic limits the number of approaches suitable for studying such molecules. Ectopic expression, which often potentiates the effect of a given protein, can result in signal inhibition by segregating signal cascade components (Burack et al., 2000 and 2001; Yasuda et al., 1999). Additionally, the high number of protein-protein interactions poses the question of which interaction is important to remove and whether it would actually result in the expected effect or just confound the results as if one were to use a dominant negative. Therefore, we have decided to begin to elucidate the function of IB2 through generation of IB2 knockout mice. Previously in our laboratory, a conditional knockout mouse was generated (Bandhyopadhyay and Goldfarb). This strategy was based on a premise that a standard knockout might be embryonic lethal due to the large number of IB2 interacting partners. My initial analysis of the conditional knockout mice using CAMKII-Cre to target postnatal deletion of *Ib2* in brain showed that CRE-mediated deletion was incomplete, leaving the animals with the functional copies of the *Ib2* gene that could be sufficient to mask phenotype. Therefore, we went on to generate the full IB2 knockout mice through the injections of the *Cre* recombinase plasmid DNA into one cell stage fertilized eggs (Kevin Kelley, Mount Sinai School of Medicine). Derived knockout mice were validated for germline knockout of the *Ib2* gene and normal expression of neighboring genes, including *Shank3* (Chapter 3).

Some of my research employed the *Ib2* knockout mice to explore whether IB2 indeed functions as a MAPK scaffold protein. However, these approaches were unproductive (Chapter 5). Far greater progress was made through unbiased biochemical and behavioral analyses of these mutant mice. I will gear my discussion towards further directions IB2 research can take based upon my findings.

Potential Functions of IB2 at the Postsynaptic Density

Using newly raised anti-IB2 antibodies, we have demonstrated that IB2 is enriched in the postsynaptic density fraction of brain extracts. In the mature hippocampal neurons, IB2 was shown by immunofluorescence to localize at bulbous caps of dendritic spines where postsynaptic densities reside. IB2 was also observed in puncta along the dendritic shaft, suggestive of active trafficking to synapses. Previously, IB2 expressed in the insulinoma cells and flag-tagged IB2 expressed in CAD cells were shown to accumulate in the cytoplasm and at the tips of neuritic projections (Verhey et al., 2001; Yasuda et al., 1999), but its endogenous localization in neuronal cells was not demonstrated. IB2's presence in the spine heads raises the possibility that it may be involved in regulating synaptic structure, transmission or plasticity.

Total levels of NMDA and AMPA receptor subunits as well as structural proteins such as PSD95 (Fig. 5-6) and SHANK3 (data not shown) are unaffected in IB2 mutant mice. Size and morphology of the synapses examined at the granule and molecular layers by our collaborator Victor Friedrich (Mount Sinai School of Medicine) also do not differ. It is possible, however, that in the absence of IB2, the PSD components are expressed at the right levels, but are mislocalized. In order to answer this question, it could be very helpful to

perform immunoelectron microscopy to analyze the spatial distribution of neurotransmitter receptors along the PSD in the IB2 knockout mice. Altered distribution of, for example, glutamate receptors could have substantial impact on synaptic transmission.

Alternatively, the levels of other postsynaptic proteins that we have not taken into consideration could be affected by the loss of IB2. A large proteomic study conducted by Collins et al. in 2006 using mass spectrometry and immunoblotting identified over one thousand distinct proteins present within the mouse postsynaptic proteome (PSP). This study identified JIP1, but not IB2, suggesting that the actual number of PSP components might be even higher. If mass spectrometry approach was applied, it could point to differences between IB2 wild type and knockout mice PSD composition. On a smaller scale, silver stain analysis of the PSD fractions could also indicate some differences.

On the other hand, the loss of IB2 could affect the synaptic signal transmission independent of additional differences in PSD composition. We observed no deficits in signaling from NMDARs to p38 MAPK or TIAM1 (Fig.5-8 and 5-9). This cannot exclude the possibility that IB2 affects these cascades downstream from these two binding partners, for instance by targeting signaling to specific changes in gene expression. IB2 as a putative scaffold is also present in the nucleus and we do have anecdotal evidence that its nuclear levels increase following NMDAR activation (data not shown). It should be noted that IB2 is also expressed in neurons such as Purkinje cells that may lack NMDA receptors, suggesting that its role in signaling may be broader or vary depending on the molecular composition of a given synapse. Microarray analysis of the transcriptome after activation of synaptic transmission in mutant and wild type cells using KCl depolarization or electrical stimulation could indicate the genes affected by loss of IB2. Specific consideration to NMDAR signaling through NMDA or glutamate stimulation in presence or absence of their blockers could also

be examined. Since nearly all identified IB2-interacting proteins reside at the synapse, including TIAM1, MAPKs, amyloid β precursor protein, and apolipoprotein receptor E2, there are many potential roles for IB2 in synaptic signaling.

Further examination of synaptic IB2 function must also include electrophysiological analyses. In fact, electrophysiology recordings performed by our collaborators Francesca Pestori and Egidio d'Angelo (University of Pavia) have revealed increased stimulus-evoked postsynaptic NMDA receptor currents at the mossy fiber - granule cell synapse in IB2-knockout cerebellum. This enhanced synaptic current could point to increased or altered distribution of NMDARs at the synapse, or may reflect a change in NMDAR channel conductivity as a consequence of IB2-mediated kinase signaling. NMDAR phosphorylation at various cytoplasmic tail residues has been shown to alter single channel conductance (Salter et al., 2009). Roger Davis' lab has analyzed JIP1/IB2 double knockout mice and found that immature cerebellar granule neurons displayed reduced nonsynaptic NMDAR currents which they attributed to reduced c-Fyn-mediated NR2B phosphorylation at Tyr1472 (Kennedy et al., 2007). I have not seen any differences in NR2B Tyr1472 phosphorylation in brain extracts from IB2 knockout mice at different developmental stages (P1, P14, and P60) (data not shown). Furthermore, our collaborators' findings indicate enhanced (synaptic), not reduced, NMDA currents in the IB2 knockout. IB2 and its protein relative JIP1 may exert multiple effects on NMDA conductances at different developmental stages and in different subcellular compartments.

Before any additional searches for synaptic signaling deficits in IB2-knockout brain, it may be helpful to identify additional proteins that directly interact with IB2. This could be tested through ectopic coexpression of IB2 and single PSD components and testing for their direct association.

Potential Roles of IB2 in Synaptic Plasticity

As a component of the postsynaptic density, IB2 may also be utilized during synaptic plasticity, affecting short- or long-lasting LTP or LTD. The most cogent argument in favor of this link comes from recent analysis of glutamatergic transmission at the cerebellar mossy fiber – granule cell synapse, which has shown substantially elevated evoked NMDA currents in the mutant (collaborators F. Prestori and E. D’Angelo, unpublished data). Since NMDA-mediated postsynaptic calcium levels are the prime determinant of LTP vs. LTD, it is possible that mutant mice will display enhanced LTP at the expense of LTD. Additional speculation on IB2 and synaptic plasticity is based upon the known functions of IB2 binding partners. The IB2 interacting protein p38 α and its upstream activators GRF1 and GRF2 are known to participate in LTD and LTP events (Li et al., 2006). This p38-dependent plasticity can be induced by exposing mice to enriched sensorimotor environment early in their development. It could be of interest to examine whether environment-triggered plasticity is impaired in IB2 mutant mice.

Another IB2-interacting protein, TIAM1, also plays roles in dendrite and dendritic spine morphological changes during development and during late-phase LTP. TIAM knockdown in cultured hippocampal neurons impairs dendritic branching and dendritic spine maturation (Tolias et al., 2005). Recent data from morphological analysis of Purkinje neurons in IB2 mutant mice did not show alterations in dendrite arborization or spine density, although a decrease in dendrite surface area and intracellular volume was detected (M. Urbanski and M. Goldfarb, unpublished data). These data do not support a clear functional link between TIAM1 and IB2, but cannot be taken as definitive. TIAM-like dendritic morphological deficits in IB2 knockouts may be found in future analysis of other brain

regions, including hippocampus. To facilitate such analysis, it would be valuable to cross the IB2 knockout mutation into transgenic Thy1-GFP mice that express GFP in small subsets of neurons, allowing for more rapid and precise cellular morphology studies (Feng et al., 2000).

Potential Functions of IB2 Beyond the Postsynaptic Density

Other roles of IB2 in neuronal transmission are suggested by IB2's known association with FHF. FHF have been found to regulate neuronal intrinsic excitability through their interaction with voltage-gated sodium channels (Goldfarb et al., 2007). Our laboratory showed that FHF binding to IB2 and sodium channels is mutually exclusive (Goldfarb and Shtraizent, unpublished data). Consistent with this finding, I have not seen IB2 at the axon initial segment of hippocampal neurons where sodium channels and FHF are concentrated.

It can be speculated that FHF facilitate IB2-mediated phosphorylation events. Prior work showed that in presence of FHF, p38 δ binds to IB2 and is activated in an FHF dose dependent manner (Schoorlemmer and Goldfarb, 2002). Unfortunately, neuronal expression and distribution of p38 δ has not been examined. In addition to p38 δ regulation, increased ERK activation is observed in FHF4 (FGF14) knockout mice (Wang et al., 2002), a signaling pathway that we did not consider in our analysis. It could be worthwhile to look for IB2 and ERK association and ERK induction in IB2 knockout mice.

Interestingly, FHF have also been shown to affect the frequency of spontaneous vesicle release, so called miniature EPSPs (Wang et al. 2002). This FHF function is independent of sodium channels and is thereby a candidate for IB2 involvement. It would be worthwhile to assay for the frequency of mEPSPs at synapses in IB2 knockout brain. Another possible function for IB2-FHF association may relate to IB2's known interaction

with the motor protein kinesin. In principle, IB2 may assist as a carrier for FHF long range transport. For example, the deficits in the grip strength observed early in development in our IB2 knockout mice could result from the failure to quickly deliver FHF to sodium channels along the nerves and near motor terminals. This could result in the impairment of neuronal firing and signal transmission from nerve to muscle early in development. Later, these deficits may be corrected by alternative FHF delivery mechanisms. In principle, this hypothesis could be tested by both FHF immunofluorescence analyses and electrophysiological recordings along nerve fibers.

Clinical Implications of the IB2 Knockout Behavioral Phenotype

Behavioral deficits in IB2 knockout mice closely phenocopy the human Phelan McDermid Syndrome in humans, which falls within the broad classification of autism spectrum disorders (Phelippe et al., 2008). These mouse deficits include reduced social interactions in juvenile IB2 knockout mice, significant motor learning deficits, developmental delay in grip strength, and frequently observed nonresponsiveness to novel environment (Chapter 4). The human *Ib2* gene resides at the terminal region of chromosome 22, only 65 kbp away from the neighboring gene *Shank3* that has been implicated in this disorder (Wilson et al., 2003). SHANK proteins play a structural role in organizing PSD components and linking them together (Sheng, 2000), but the phenotype of a SHANK3 knockout mouse model has not been described. In nearly all analyzed human patients with this syndrome, the *Ib2* gene is also deleted. The size of the deletion does not correlate with the profoundness of the phenotype (Wilson et al., 2003). Nevertheless, the lack of both SHANK3 and IB2 protein could have a synergistic impact on synaptic functioning.

The IB2 mutant phenotype, although highly suggestive of an autism-like behavior, could be open to alternative interpretations. Additional behavioral analysis of our mutant animals could help clear up some of these doubts and strengthen IB2 knockout as a clinical candidate model of autism. For instance, it would be very interesting to monitor IB2 knockout mice performance in their home cage by examining interactions with their parents and unaffected littermates (Crawley, 2007). Another interesting aspect of IB2 mutant mice, which we have not examined further, is their extremely poor breeding performance and inability to care for many offspring. Their ability to give progeny argues against their infertility and suggests that these deficits may stem from autistic-like behavioral disturbances. Lastly, we have not tested another very interesting feature of autism and Phelan McDermid syndrome, which is a skill loss or inability to maintain acquired or learned behavior. It would be interesting to determine a task in which IB2 mice are able to learn and then to re-examine their performance after a certain period of to test whether they were able to retain this memory.

Additionally, I have not analyzed closely the phenotype of mice heterozygous for the IB2 mutation. Hemizyosity might result in an intermediate phenotype between wild-type and null, particularly for behaviors in which IB2 knockout mice were strongly affected. Since 22q13 Syndrome usually features chromosome deletions resulting in hemizyosity for a cluster of linked genes, it will be very important to analyze the behavior of mice that are hemizygous for *Ib2* and neighboring genes. Of particular interest would be an *Ib2/Shank3* double heterozygote, given the central role attributed to SHANK3 in the human syndrome. As several laboratories now have *Shank3* mutant mice (SFN Neuroscience 2009 meeting), generation of such double heterozygotes is straightforward. If *Ib2/Shank3* double heterozygotes do not have clear behavioral deficits, it could be necessary to mimic the human

deletion by generating a corresponding regional deletion of the syntenic portion of mouse chromosome 15. Assuming that the larger deletion generates autistic-like deficits, the contribution of particular genes within the deleted region could be assessed by transgenic reintroduction of an extra copy of a particular gene, including *Ib2*. This approach was successfully used to determine the critical role of the *MecP2* gene in Rett's syndrome (Guy et al., 2007).

Furthermore, the direct link between IB2 and human ASDs could be explored by obtaining blood and tissue samples from individuals with autism and from unaffected relatives. DNA from such samples could be screened for mutations in the *Ib2* gene. Furthermore, even though autism has many separate genetic causes, they could converge on the proper expression of a particular set of genes, including *Ib2*, at the RNA or protein levels. Perhaps the most sensitive test would be to examine PSDs prepared from biopsy or post-mortem autistic brain tissue for altered abundance of IB2. Our hope is for IB2 mutant mice to emerge as a clinical model for autism and serve as a tool for rescue strategies through gene therapy and possible therapeutics based upon IB2 mechanism of action.

Bibliography:

Bourne J.N. and K.H. Harris. 2007. Dendritic Spines. *Encyclopedia of Life Sciences*. 1-7

Bourne J.N. and K.H. Harris. 2008. Balancing Structure and Function at Hippocampal Dendritic Spines. *Annu Rev Neurosci*. 31:47-67.

Buchsbaum R.J., Conolly B.A., Feig L.A. 2002. Interaction of Rac Exchange Factors Tiam1 and Ras-GRF1 with a Scaffold for the p38 Mitogen-Activated Protein Kinase Cascade. *Mol Cell Biol*. 22:4073-4085.

Burack W.R., Cheng A.M., Shaw A.S. 2002. Scaffolds, adaptors and linkers of TCR signaling: theory and practice. *Curr Opin Immunol*. 14:312-316

Burack W.R. and A.S. Shaw. 2000. Signal transduction: hanging on a scaffold. *Curr Opin Cell Biol*. 12:211-216

Chao H-T., Zoghbi H.Y., Rosenmund C. 2007. MeCP2 Controls Excitatory Synaptic Strength by Regulating Glutamatergic Synapse Number. *Neuron*. 56: 58-65.

Crawley J.N. 2007. Mouse Behavioral Assays Relevant to the Symptoms of Autism. *Brain Pathology*. 448-459.

Diagnostic and statistical manual of mental disorders: *DSM-IV*

Dragatsis I and S. Zeitlin. 2000. CaMKIIalpha-Cre transgene expression and recombination patterns in the mouse brain. *Genesis*. 26:133-135

Echeverry M.B., Hasenohrl R.U., Huston J.P., Tomaz C. 2001. Comparison of neurokinin SP with diazepam in effects on memory and fear parameters in the elevated T-maze free exploration paradigm. *Peptides*.22:1031-1026.

Elion EA. 2001. The Ste5p scaffold. *J Cell Sci*. 114: 3967-78

Feng G., Hood, R., Bernstein, M., Keller-Peck, C., Nguyen, Q., Wallace, M., Nerbonne, J.M., Lichtman, J.W. and Sanes, J.R (2000). Imaging neuronal subsets in transgenic mice expressing multiple spectral variants of GFP. *Neuron* 28:41-51.

Ferrell JE. 2000. What do scaffold proteins really do? *Perspective*. 1-3.

Flatauer L.J., Zadeh S.F., Bardwell L. 2005. Mitogen-Activated Protein Kinases with Distinct Requirements for Ste5 Scaffolding Influence Signaling Specificity in *Saccharomyces Cerevisiae*. *Molec and Cell Biol.* 25: 1793-1803.

Gallo K. A. and G.L. Johnson. 2002. Mixed-lineage kinase control of JNK and p38 MAPK pathways. *Nature Reviews.* 3: 663-672.

Garner C. and J. Nash. 2001. Chemical Synapses. *Encyclopedia of Life Sciences.* 1-8.

Goldfarb, M., Schoorlemmer, J., Williams, A., Diwakar, S., Wang, Q., Huang, X., Giza, J., Tchetchik, D., Kelley, K., Vega, A., Matthews, G., Rossi, P., Ornitz, D.M., and D'Angelo, E. 2007. Fibroblast growth factor homologous factors control neuronal excitability through modulation of voltage-gated sodium channels. *Neuron* 55, 449-463.

Good M., Tang G., Singleton J., Remenyi A., Lim W.A. 2009. The Ste5 Scaffold Directs Mating Signaling by Catalytically Unlocking the Fus3 MAPK for Activation. *Cell.* 136:1085-97.

Guy J., Gun J., Selfridge J., Cobb S., Bird A. 2007. Reversal of Neurological Defect in a

Mouse Model of Rett Syndrome. *Science*. 315:1143-1147.

Hascoët M., Bourin M., Dhonnchadha B.A. 2001. The mouse light-dark paradigm: a review.

Prog Neuropsychopharmacol Biol Psychiatry. 25(1):141-66.

Hung A., Futai K., Sala C., Valtschanoff J.G., Ryu J., Woodworth M.A., Kidd F.L., Sung

C.C., Miyakawa T., Bear M.F., Weinberg R.J., Sheng M. 2008. Smaller Dendritic

Spines, Weaker Synaptic Transmission, but Enhanced Spatial Learning in Mice

Lacking Shank1. *J Neurosci*.28:1697-1708.

Jardim M.C., Nogueira R.L., Graeff F.G., Nunes-de-Souza R.L. 1999. Evaluation of the

elevated T-maze as an animal model of anxiety in the mouse. *Brain Res*. 4:407-

411.

Johnson G.L. and R. Lapadat. 2002. Mitogen-Activated Protein Kinase Pathways Mediated

By ERK, JNK, and p38 Protein Kinases. *Science*. 298: 1911-1912

Kandel E.R., Schwartz J.H., Jessell T.M. 2000. Principles of Neural Science. 4th edition.

Kelkar N., Standen C.L. , Davis R.J. 2005. Role of JIP4 Scaffold Protein in the Regulation of

Mitogen Activated Protein Kinase Signaling Pathways. *Molec and Cell Biol*.

Kennedy NJ, Martin G, Ehrhardt AG, Cavanagh-Kyros J, Kuan CY, Rakic P, Flavell RA, Treisman SN, Davis RJ. 2007. Requirement of JIP scaffold proteins for NMDA-mediated signal transduction. *Genes Dev.* 2007 Sep 15;21(18):2336-46.

Li S. Tian X., Hartley D.M., Feig L.A. 2006 A. Distinct Roles for Ras-Guanine Nucleotide-Releasing Factor 1 (Ras-GRF1) and Ras-GRF2 in the Induction of Long-Term Potentiation and Long-Term Depression. *J Neurosci.* 26:1721-29.

Li S. Tian X., Hartley D.M., Feig L.A. 2006 B. The Environment versus Genetics in Controlling the Contribution of MAP Kinases to Synaptic Plasticity. *Curr Biol.* 16:2303-2313.

Negri S., Oberson A., Steinmann M., Sauser Ch., Nicod P., Waeber G., Schorderet D.F., Bony Ch. 2000. cDNA Cloning and Mapping of a Novel Islet-Brain/JNK-Interacting Protein. *Genomics.* 64:324-330.

Philippe A., Boddaert N., Vaivre-Douret L., Robel L., Danon-Boileau L., Malan V., de Blois M C., Heron D., Colleaux L., Golse B., Zilbovicius M., Munnich A. 2008. Neurobehavioral profile and Brain Imaging Study of the 22q13.3 Deletion Syndrome

in *Children.Pediatrics*. 276-382.

Robidoux J., Cao W., Quan H., Daniel K.W., Moukdar F., Bai X., Floering L.M.,

Collins S. 2005. Selective activation of mitogen-activated protein (MAP) kinase kinase 3 and p38 α MAP kinase is essential for cyclic AMP-dependent UCP1 expression in adipocytes.

Roux P.P and J. Blenis. 2004. ERK and p38MAPK-activated Protein Kinases: a Family of

Protein Kinases with Diverse Biological Functions. *Microbiol Mol Biol Rev*.68:320-344

Salter MW, Dong Y, Kalia LV, Liu XJ, Pitcher G. 2009. Regulation of NMDA Receptors by

Kinases and Phosphatases. *Biology of NMDA receptor. Frontiers in Neuroscience*.

Schoorlemmer, J., and M. Goldfarb. 2001. Fibroblast growth factor homologous factors

are intracellular signaling proteins. *Curr Biol*. 11:793-7.

Schoorlemmer, J., and M. Goldfarb. 2002. Fibroblast growth factor homologous factors

and the Islet Brain-2 Protein Regulate Activation of a Stress-activated Protein

- Kinase. *J Biol Chem.* 277:49111-49119.
- Sevin C., Verot A., Benraiss A., Van Dam D., Bonnin D., Nagles G., Fouquet F., Gieselmann V., Vanier M.T., De Deyn P.P., Aubourg P., Cartier N. 2007. Partial cure established disease in an animal model of metachromatic leukodystrophy after intracerebral adeno associated virus-mediated gene transfer. *Gene Therapy.* 14:405-414.
- Sheng M. and E.Kim. 2000. The Shank family of scaffold proteins. *J Cell Sci.* 113:1851-56.
- Stockinger W., Brandes C., Fasching D., Hermann M., Gotthardt M., Herz J., Schneider W.J., Nimpf J. 2000. The Reelin receptor ApoER2 recruits JNK-interacting Proteins-1 and -2. *J Biol Chem.* 275:25625-25632.
- Tabuchi K., Blundell J., Etherton M. R., Hammer R.E. Liu X., Powell C.M. Sudhof T.C. 2007. A Neuroligin-3 Mutation Implicated in Autism Increases Inhibitory Synaptic Transmission in Mice. *Science.* 318: 71-76
- Takeda K. and H.Ichijio. 2002. Neuronal p38 MAPK signaling: an emerging regulator

- of cell fate and function in the nervous system. *Genes to Cells*. 7:1099-1111.
- Tanoue T. and E. Nishida . 2003. Molecular recognitions in the MAP kinase cascades. *Cellular Signalling* . 15: 455–462
- Tolias K.F., Bikoff J.B., Burette A., Paradis S., Harrar D., Tavazoie S., Weinberg R.J., Greenberg M.E. 2005. *Neuron*. 45:525-538.
- Verhey K.J., Meyer D., Deehan R., Blenis J., Schnapp B.J., Rapport T.A., Margolis B. 2001. Cargo of Kinesin Identified as JIP Scaffolding Proteins and Associated Signaling Molecules. *J Cell Biol* 152:956-970.
- Walsh C.A., Morrow E.M., Rubenstein J.L.R. 2008. Autism and Brain Development. *Cell*. 135: 396-400.
- Wang Q., Bardgett M.E., Wong M., Wozniak D.F., Lou J., McNeil B.D., Chen C., Nardi A., Reid D.C., Yamada K., Ornitz D. M. 2002. Ataxia and paroxysmal dyskinesia in mice lacking axonally transported FGF14. *Neuron*. 35:25-38.
- Whitmarsh A.J., Kwan C., Kennedy N.J., Kelkar N., Haydar T.F., Mordes J.P., Appel M., Rossini A.A., Jones S.N., Flavell R.A., Rakic P., Davis R.J. 2001. Requirement

of the JIP1 scaffold protein for stress-induced JNK activation. *Genes&Dev.*
15:2421-2432.

Wilson H.L., Wong A.C.C., Shaw S.R., Tse W-Y., Stapleton G.A., Phelan M.C., Hu S.,
Marshall J., McDermid H.E. 2003. Molecular characterization of the 22q13
deletion syndrome supports the role of haploinsufficiency of SHANK3/PROSAP2
in the major neurological symptoms. *J. Med. Genet.* 40:575-584.

Wozniak D.F., Brosnan-Watters G., Nardi A., McEwen M., Corso T.D., Olney J.W.,
Fix A.S. 1996. MK-801 neurotoxicity in male mice: histologic effects and chronic
impairment in spatial learning. *Brain Res.* 707:165-179.

Wu G., Sher I.B., Cox G.A., Vance D.E. 2009. Understanding the muscular dystrophy caused
by deletion of choline kinase beta in mice. *Biochim Biophys Acta.* 1791:347-56

Yasuda J., Whitmarsh A.J., Cavanagh J., Sharma M., Davis R.J. 1999. The JIP Group of
Mitogen-Activated Protein Kinase Scaffold Proteins. *Mol Cell Biol.* 19:7245-
7254.

Zoghbi H.Y. 2003. Postnatal Neurodevelopmental Disorders: Meeting at the Synapse?

Science.302:826-830.